ELSEVIER

CYTOKINE

www.elsevier.com/locate/jnlabr/ycyto

Cytokine 24 (2003) 293–303

The negative-feedback regulation of the IL-13 signal by the IL-13 receptor α2 chain in bronchial epithelial cells

Shin,ichiro Yasunaga[a,1], Noriko Yuyama[b,1], Kazuhiko Arima[a,1], Hiroyuki Tanaka[c], Shuji Toda[d], Miyako Maeda[b], Keiko Matsui[b], Chiho Goda[a], Qing Yang[a,2], Yuji Sugita[b], Hiroichi Nagai[c], Kenji Izuhara[a,e,*]

[a]*Division of Medical Biochemistry, Department of Biomolecular Sciences, Saga Medical School, 5-1-1, Nabeshima, Saga 849-8501, Japan*
[b]*Genox Research, Inc., Kawasaki, Japan*
[c]*Department of Pharmacology, Gifu Pharmaceutical University, Gifu, Japan*
[d]*Division of Cellular & Molecular Pathology, Department of Pathology & Biodefence, Saga Medical School, Saga, Japan*
[e]*Division of Medical Research, Center for Comprehensive Community Medicine, Saga Medical School, Saga, Japan*

Received 1 January 2003; received in revised form 2 August 2003; accepted 12 August 2003

Abstract

Bronchial asthma is a complex disease characterized by airway inflammation involving Th2 cytokines. Among Th2 cytokines, the significance of IL-13 in the pathogenesis of bronchial asthma has recently emerged. Particularly, the direct action of IL-13 on bronchial epithelial cells (BECs) is critical for generation of airway hyperresponsiveness. IL-13 has two binding units; the IL-13 receptor α1 chain transduces the IL-13 signal comprising a heterodimer with the IL-4R α chain, whereas the IL-13 receptor α2 chain (IL-13Rα2) is thought to act as a decoy receptor. However, it remains obscure how expression of these molecules is regulated in each cell. In this article, we analyzed the expression of these components in BECs. Either IL-4 or IL-13 induced intracellular expression of IL-13Rα2 in BECs, which was STAT6-dependent and required de novo protein synthesis. IL-13Rα2 expressed on the cell surface as a monomer inhibited the STAT6-dependent IL-13 signal. Furthermore, expression of IL-13Rα2 was induced in lung tissues of ovalbumin-induced asthma model mice. Taken together, our results suggested the possibility that IL-13Rα2 induced by its ligand is transferred to the cell surface by an unknown mechanism, and it down-regulates the IL-13 signal in BECs, which functions as a unique negative-feedback system for the cytokine signal.

Keywords: Allergy; Cytokine; Cytokine receptor; Lung; Signal transduction

1. Introduction

Allergic diseases are complex disorders involving a combination of genetic and environmental factors [1]. In bronchial asthma, these factors result in infiltration of Th2 lymphocytes, mast cells, and eosinophils into lesions with a downstream mediator, leading to the formation of the asthmatic phenotypes such as mucous hyperproduction, airway hyperresponsiveness (AHR), and submucosal thickness. Cytokines derived from Th2 lymphocytes are considered to orchestrate such asthmatic phenotypes [1]. Among the Th2 cytokines, considerable evidence based on analyses of mouse models supports key roles for IL-13 in the pathogenesis of bronchial asthma; mice null for the components of the IL-13 signal transduction pathways—including IL-13, the IL-4 receptor α chain (IL-4Rα), and STAT6—showed a decrease of AHR [2–4]. Furthermore, overexpression of an IL-13 transgene on bronchial epithelial cells (BECs) or administration of IL-13 in mice induced asthma-like phenotypes independent of lymphocytes [5–7]. It is of importance to

* Corresponding author. Tel.: +81-952-34-2261; fax: +81-952-34-2058.
E-mail address: kizuhara@post.saga-med.ac.jp (K. Izuhara).
[1] These authors equally contributed to this work.
[2] Present address: Molecular Medicine Research Center, Jiangxi Medical College, Nanchang, People's Republic of China.

1043-4666/03/$ - see front matter © 2003 Elsevier Ltd. All rights reserved.
doi:10.1016/j.cyto.2003.08.006

note that these analyses indicated that IL-13 acts directly on non-immune cells in bronchial tissue, evoking the phenotypic changes. Actually, it has been very recently reported that reconstitution of STAT6 only in BECs into STAT6-disrupted mice restores IL-13-induced AHR and mucous production, but not inflammation or fibrosis [8], showing the importance of IL-13's direct action on BECs. In bronchial asthma patients, IL-13 was highly expressed at baseline and greatly up-regulated by allergen challenge in bronchial tissues or bronchoalveolar lavage fluids [9,10]. Furthermore, we recently found that a variant of *IL13* (Gln110Arg) was associated with the incidence of bronchial asthma and serum level of IL-13 [11], which would be due to low affinity of the variant with the IL-13R α2 chain (IL-13Rα2), and also due to enhanced stability of the variant compared to the wild type [12]. Such evidence supports an important role of IL-13 also for the pathogenesis of human bronchial asthma.

IL-13R is composed of two components, the IL-13R α1 chain (IL-13Rα1) and IL-4Rα, which also act as IL-4R [13,14]. Upon engagement of the receptor with IL-13, its signal is transduced mainly via the JAK–STAT pathway and the phosphatidylinositol-3 kinase/insulin receptor substrate-1/2 pathway [13,14]. IL-13 activates JAK1 and TYK2 for the JAK family, followed by activation of STAT6 and STAT3 for the STAT family [15,16]. It is well characterized that STAT6 is critical for IL-13 to exert its biological activities [13,14]. In hematopoietic and immune cells, B cells and monocytes are the main target cells for IL-13 [13]. Although IL-13Rα1 was not expressed on the cell surface at the resting stage of human B cells, activation by anti-IgM Ab and anti-CD40 Ab enhanced expression of IL-13Rα1, which enabled the cells to respond to IL-13, causing class switching to IgE and CD23 expression [16,17]. Thus, the IL-13 signal is regulated by expression of IL-13Rα1 in B cells. In contrast, we revealed that IL-13Rα1 is widely expressed in non-hematopoietic cells, including human BECs [11,18].

There exists another IL-13-binding unit, IL-13Rα2 [13,14]. The cytoplasmic domain of IL-13Rα2 is short and does not conserve the box-1 region, critical for various cytokine receptors to associate with JAK, transducing the downstream signals [19]. IL-13Rα2 has therefore been thought not to transduce the IL-13 signal, but to block it, acting as a 'decoy receptor', defined as a receptor with specificity and high affinity with ligands, but incapable of signaling. Actually, it has been recently reported that transfection of IL-13Rα2 into CHO-K1 cells already transfected with IL-13Rα1 or IL-4Rα or into renal cell carcinoma cells abrogated STAT6 activation [20,21]; however, we still cannot exclude the possibility that IL-13Rα2 could act as another IL-13R with unknown co-receptor, depending on cell type. It has been confirmed that immune cells do not express IL-13Rα2 [17]. The IL-13-binding units have been identified in this manner; however, it remains obscure how the expression of these molecules is regulated in non-immune cells such as human BECs, and how it might be correlated with the pathogenesis of bronchial asthma.

We recently identified by microarray analysis that IL-13Rα2 is one of the IL-4- or IL-13-induced genes in human BECs [22]. In the present study, we analyzed the regulation of IL-13Rα2 expression in human BECs. Intracellular expression of IL-13Rα2 was selectively induced by IL-4 or IL-13, although the copy numbers of mRNA were variable among the donors, whereas expression of neither IL-13Rα1 nor IL-4Rα is significantly influenced by IL-4 or IL-13. IL-13Rα2 induction by IL-4 or IL-13 required de novo protein synthesis and was dependent on STAT6. IL-13Rα2 was likely to act as a decoy receptor by itself alone. Furthermore, expression of IL-13Rα2 was detected in lung tissues of ovalbumin-induced asthma model mice, in which both IL-4 and IL-13 were highly expressed. These results suggested the possibility that IL-13Rα2 induced by its ligand is transferred to the cell surface by an unknown mechanism, and it down-regulates the IL-13 signal in BECs, which functions as a unique negative-feedback system for the cytokine signal.

2. Results

2.1. Induction of IL-13Rα2 mRNA by IL-4 or IL-13 in human BECs

We previously demonstrated by microarray analysis that IL-13Rα2 was one of the IL-4- or IL-13-induced genes in human BECs [22]. To confirm this, we first investigated the effects of variation of cell donors and kinetics on IL-13Rα2 induction in human BECs by quantitative RT-PCR analysis. When we incubated the cells in the presence of IL-4 or IL-13, all of the tested cells derived from seven donors expressed 3–23 fold more IL-13Rα2, although the copy numbers of mRNA were variable among the donors (9.7 ± 8.0 fold for IL-4, 11.8 ± 7.3 fold for IL-13, mean $\pm$ SD, $n = 7$, Fig. 1A, B). We confirmed that expression level of IL-13Rα2 by IL-13 was almost the same at 10 ng/ml and 50 ng/ml, indicating that these concentrations were enough for IL-13 to perform its maximum biological activity (data not shown). The kinetics analysis showed that the increase of IL-13Rα2 induction continued at least up to 48 h after the stimulation (Fig. 1C). TNF-α alone did not induce expression of IL-13Rα2; however, it had a tendency to show a slight synergistic effect with IL-4 or IL-13 (Fig. 1D). In contrast, IFN-γ inhibited IL-4- or IL-13-induced IL-13Rα2 expression (Fig. 1D). Neither IL-1β, IL-5, IL-6, or IL-9 enhanced expression of IL-13Rα2 by itself, nor did any of these cytokines show a synergistic effect with IL-4 or IL-13 (data not shown).

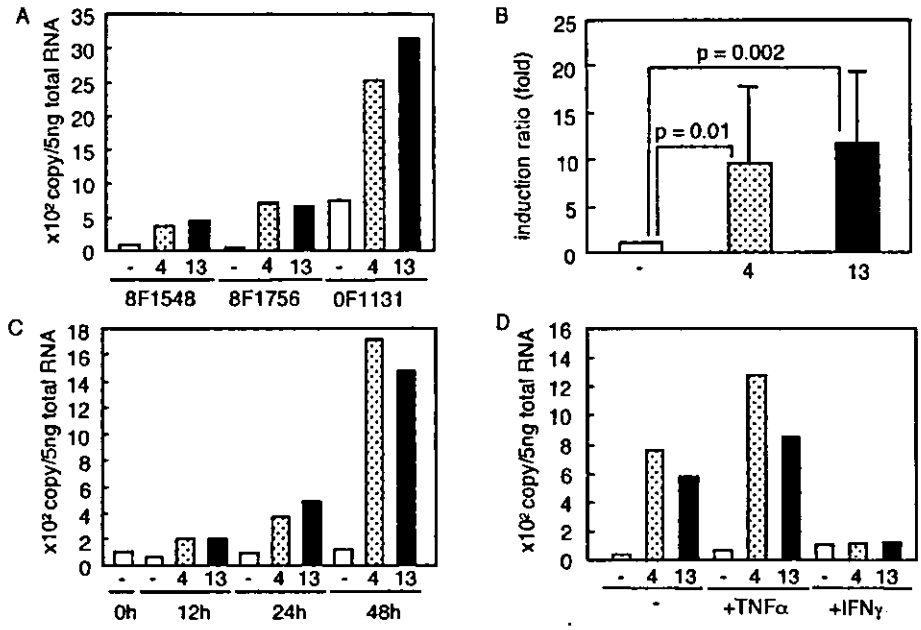

Fig. 1. mRNA expression of IL-13Rα2 in human BECs. (A) Human BECs were incubated in the absence (open bar) or presence of either 10 ng/ml of IL-4 (dotted bar) or 50 ng/ml of IL-13 (closed bar) for 24 h. Representative data derived from three different donors (8F1548, 8F1756, and 0F1131) are depicted. (B) Induction rate of IL-13Rα2 by IL-4 (dotted bar) or IL-13 (closed bar) in seven different donors as prepared in Panel (A) is depicted. (C) Human BECs (8F1548) were incubated in the absence (open bar) or presence of either 10 ng/ml of IL-4 (dotted bar) or 50 ng/ml of IL-13 (closed bar) for the indicated times. (D) Human BECs (0F0674) were incubated in the absence (open bar) or presence of either 10 ng/ml of IL-4 (dotted bar) or 50 ng/ml of IL-13 (closed bar) for 24 h in the absence or presence of either 10 ng/ml of TNF-α or IFN-γ. Expression of IL-13Rα2 was investigated by quantitative RT-PCR analysis. The copy number was calculated using a standard plasmid, and the concentration of cDNA was normalized by reference to the copy number of GAPDH. The same experiments were performed twice (C) or three times (D), and the representative data are depicted.

We next analyzed the effects of IL-4 and IL-13 on induction of two components of the IL-13R, IL-13Rα1 and IL-4Rα (Fig. 2). The expression level of both IL-13Rα1 and IL-4Rα by IL-4 or IL-13 was variable among donors; however, it was within 2 fold, indicating that expression of neither IL-13Rα1 nor IL-4Rα is significantly influenced by IL-4 or IL-13. Neither TNF-α nor IFN-γ had an effect on it (data not shown). These results clearly demonstrate that IL-4 and IL-13 up-regulate IL-13Rα2 mRNA selectively, among the IL-13-binding components in human BECs.

2.2. Induction of IL-13Rα2 protein by IL-4 or IL-13 in human BECs

To address whether IL-4 or IL-13 induces IL-13Rα2 expression in human BECs, not only at the mRNA level, but also at the protein level, we next performed immunostaining of IL-13Rα2 in human BECs. When human BECs were incubated with either IL-4 or IL-13, staining of IL-13Rα2 was observed ubiquitously inside the cell, whereas the cells without the stimulant did not elicit staining (Fig. 3A). Again, neither IL-4 nor IL-13 affected IL-13Rα1 expression (Fig. 3B). However, expression of IL-13Rα2 on the cell surface was not detected by flow cytometry in the stimulated cells (data not shown). These results demonstrate that synthesis of IL-13Rα2 protein is up-regulated by IL-4 or IL-13 in human BECs in parallel with its mRNA expression.

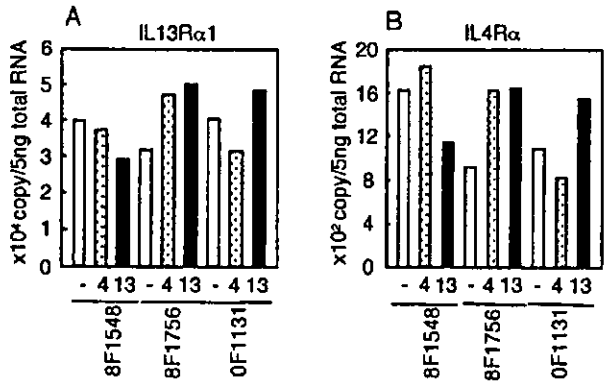

Fig. 2. mRNA expression of IL-13Rα1 and IL-4Rα in human BECs. Human BECs derived from three different donors (8F1548, 8F1756, and 0F1131) were incubated in the absence (open bar) or presence of either 10 ng/ml of IL-4 (dotted bar) or 50 ng/ml of IL-13 (closed bar) for 24 h. Expression of IL-13Rα1 (A) or IL-4Rα (B) was investigated by quantitative RT-PCR analysis, as described in Fig. 1.

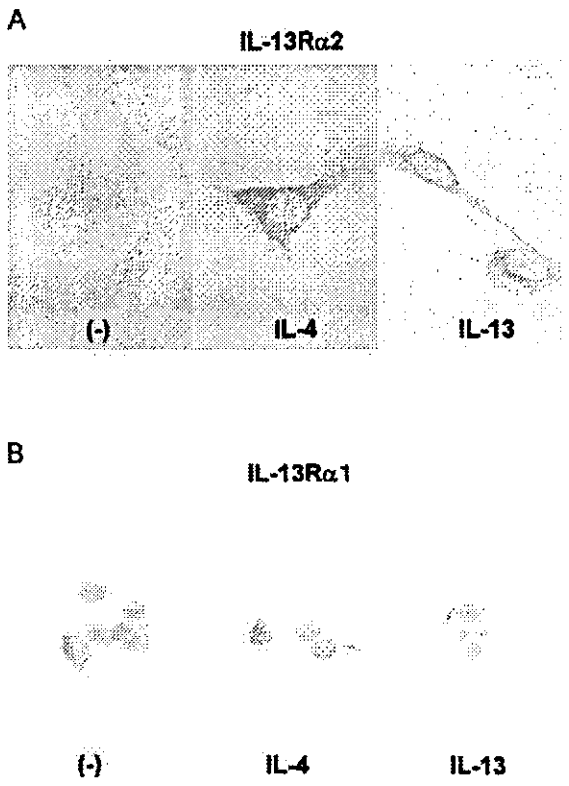

Fig. 3. Protein expression of IL-13Rα1 and IL-13Rα2 in human BECs. Human BECs were incubated in the absence (left panel) or presence of either IL-4 (middle panel) or IL-13 (right panel). Immunostaining was performed using anti-IL-13Rα2 Ab (A) or an anti-IL-13Rα1 Ab (B).

2.3. Expression mechanism of IL-13Rα2 induction by IL-4 or IL-13 in BECs

The finding that mRNA induction of IL-13Rα2 was relatively slow (Fig. 1C) raised the possibility that IL-4 or IL-13 did not directly elicit IL-13Rα2 expression, but did it through de novo protein synthesis. To explore this, we tested the effects of cycloheximide on enhancement of IL-13Rα2 expression by IL-4 or IL-13. For this purpose, we used a mouse tracheal epithelial cell line, TGMBE-02-3 cells, because this cell line responded to murine IL-4 or IL-13, leading to IL-13Rα2 mRNA induction as well as human BECs (Fig. 4A). The other cell lines that we tested, such as BEAS-2B and A549, did not express increased levels of IL-13Rα2 upon stimulation with IL-4 or IL-13 (data not shown). When the cells were cultured in the presence of cycloheximide, induction of IL-13Rα2 but not eotaxin was attenuated in a dose-dependent manner (Fig. 4B). These results indicate that IL-4 and IL-13 would generate some proteins—probably some secreted protein or some transcriptional factor—through which expression of IL-13Rα2 would be induced.

It is widely known that STAT6 is a critical transcriptional factor for IL-4 and IL-13 to exert their biological activities [13,14]. Although the actions of IL-4 and IL-13

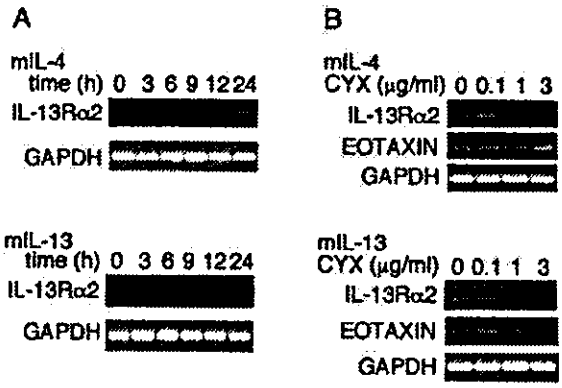

Fig. 4. Expression of IL-13Rα2 in TGMBE-02-3 cells and effects of cycloheximide on it. (A) TGMBE-02-3 cells were incubated in the absence or presence of either 10 ng/ml of IL-4 or 50 ng/ml of IL-13 for the indicated periods. (B) TGMBE-02-3 cells were preincubated in the absence or presence of the indicated concentrations of cycloheximide for 30 min, and then incubated with either 10 ng/ml of IL-4 or 50 ng/ml of IL-13 for 9 h. Expression of IL-13Rα2 and eotaxin was analyzed by RT-PCR.

on IL-13Rα2 induction would be indirect, it would be possible that STAT6 locates at the upstream of the signal pathway for the transcription of IL-13Rα2, thereby controlling it. To address this question, we generated TGMBE-02-3 cells expressing the truncated STAT6. Dominant negative effects of the transfected truncated STAT6 were confirmed by diminishment of the binding of nuclear extract to the STAT6 binding sequence by electrophoretic mobility shift assay (EMSA) (Fig. 5A). When the transfectants were incubated with either IL-4 or IL-13, expression of both IL-13Rα2 and eotaxin declined, compared to parental or mock-transfected cells (Fig. 5B). Taken together, these findings show that activated STAT6 by IL-4 or IL-13 would not directly induce IL-13Rα2 expression, but an unknown secreted protein or an unknown transcriptional factor induced by STAT6 would express IL-13Rα2.

2.4. Functional analysis of IL-13Rα2 as a 'decoy receptor'

IL-13Rα2 is thought to act as a 'decoy receptor', not transducing the IL-13 signal, but blocking it. It has been reported that transfection of IL-13Rα2 into some cells abrogated the IL-13 signal [20,21]. To study whether this is also the case in human BECs, we stably transfected IL-13Rα2 into BEAS-2B cells, and analyzed STAT6 phosphorylation induced by IL-4 and IL-13. The expression of the transfected IL-13Rα2 on the cell surface was confirmed by flow cytometry (Fig. 6A). In the mock-transfected cells, both IL-4 and IL-13 caused STAT6 phosphorylation (Fig. 6B), meaning that this cell line expressed functional IL-13R. IL-13 completely diminished STAT6 phosphorylation in the IL-13Rα2-expressing cells, whereas IL-4 did not influence it (Fig. 6B).

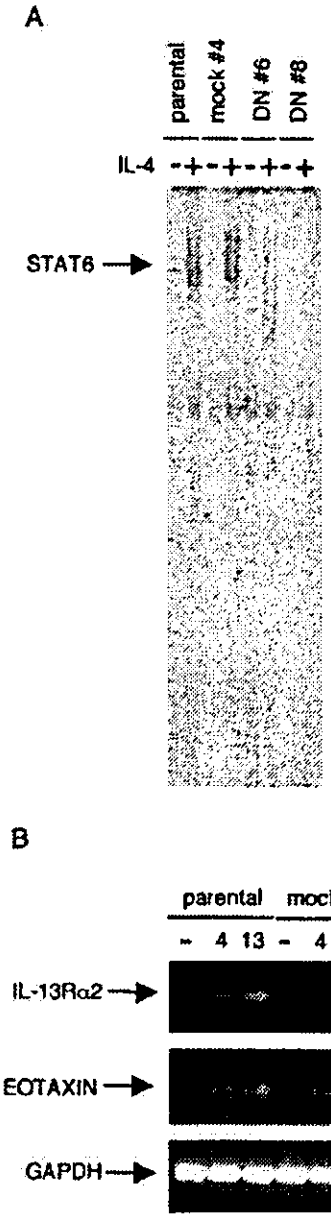

Fig. 5. Expression of IL-13Rα2 in TGMBE-02-3 cells expressing the truncated STAT6. Parental or mock-transfected or the truncated STAT6-transfected (DN) TGMBE-02-3 cells were incubated in the absence or presence of either 10 ng/ml of IL-4 or 50 ng/ml of IL-13 for 24 h. (A) Activation of STAT6 was analyzed by EMSA. (B) Expression of IL-13Rα2 and eotaxin was analyzed by RT-PCR.

Transfection of IL-13Rα2 into a human Burkitt cell line, DND-39 cells, also led to down-regulation of STAT6 phosphorylation (data not shown). These results demonstrated that IL-13Rα2 selectively inhibited the STAT6-dependent IL-13 signal in HBECs.

To explore the possibility that IL-13Rα2 is involved in the formation of oligomer complex with an unknown component in human BECs, we performed chemical cross-linking experiments using radiolabeled IL-13. The

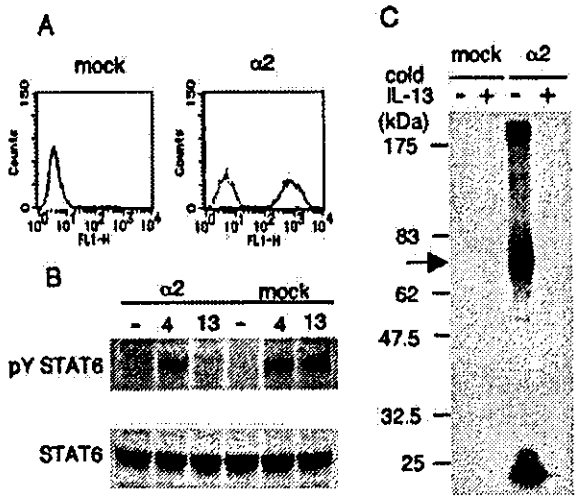

Fig. 6. Functional analysis of IL-13Rα2. (A) Expression of IL-13Rα2 on mock-transfected or IL-13Rα2-transfected BEAS-2B cells was analyzed by flow cytometry using anti-IL-13Rα2 Ab. (B) Cell lysates stimulated by 10 ng/ml of IL-4 or IL-13 for 10 min at 37 °C of mock-transfected or IL-13Rα2-transfected BEAS-2B cells were probed with anti-phospho STAT6 Ab or anti-STAT6 Ab. (C) Cross-linked cell lysates of mock-transfected or IL-13Rα2-transfected BEAS-2B cells with radiolabeled IL-13 were subjected to SDS-PAGE and autoradiography.

cross-linking of radiolabeled IL-13 on the IL-13Rα2-expressing cells showed only a single band with ~70 kDa, corresponding to the molecular size of the IL-13/IL-13Rα2 complex, indicating that IL-13Rα2 would act as a monomer on human BECs (Fig. 6C). We still cannot exclude the possibility that IL-13Rα2 is capable of transducing certain STAT6-independent IL-13 signals; however, the present results strongly suggest that IL-13Rα2 induction leads to inhibition of the IL-13 signal transduced through the IL-4Rα/IL-13Rα1 receptor.

2.5. Augmentation of IL-13Rα2 expression in mouse model of bronchial asthma

To address whether the results of the in vitro analysis that we performed reflect the in vivo events, we next employed mice in which bronchial asthma was triggered by ovalbumin inhalation. It has been already shown that asthma-like characteristics such as mucous overproduction, eosinophil infiltration, airway hypersensitivity, and submucosal fibrosis occur upon ovalbumin inhalation in this model, with dominant expression of Th2 cytokines including IL-4 and IL-13 in bronchial lesions [23]. We analyzed expression of IL-13Rα1, IL-13Rα2, and IL-4Rα by quantitative RT-PCR in lung tissues of four groups of mice: (1) naive, (2) saline inhalation, (3) ovalbumin inhalation, and (4) ovalbumin inhalation and oral prednisolone intake. Expression of IL-13Rα2 was not detected in naive and saline inhalation groups; however, it was significantly enhanced in the ovalbumin

inhalation group and declined in the presence of prednisolone (Fig. 7A). In contrast, expression of both IL-13Rα1 and IL-4Rα was constitutive, and the expression level was invariable in the four groups (Fig. 7B and C). Expression of IL-13Rα2 after the first ovalbumin inhalation was lower than after the third inhalation, although two rounds of inhalations had almost the same effect as three (Fig. 7D). We confirmed the appearance of the asthmatic phenotypes and the up-regulation of IL-4/IL-13 production in the bronchial lesions by ovalbumin inhalation and their relief by prednisolone as previously reported (data not shown). It would be possible that not only BECs but also other cells such as fibroblasts expressed IL-13Rα2 in the asthmatic condition, reflecting high induction of IL-13Rα2 in this analysis; however, these results strongly support that IL-13Rα2, but not IL-13Rα1 and IL-4Rα, is profoundly expressed in asthmatic conditions, and that IL-4 and IL-13 would be involved in this event.

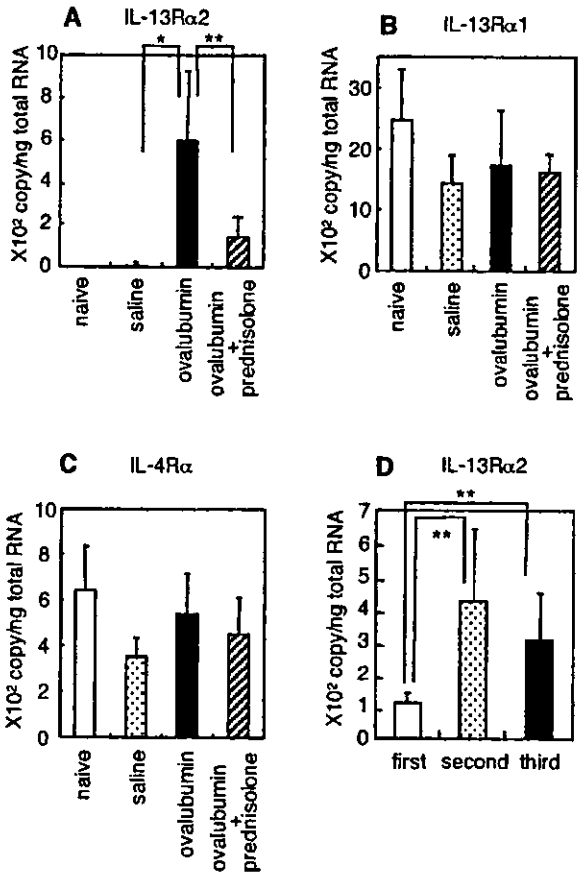

Fig. 7. mRNA expression of the receptor components in bronchial asthma model mice. (A–C) mRNA expression of IL-13Rα2, IL-13Rα1, and IL-4Rα was investigated by quantitative RT-PCR analysis, as described in Fig. 1, in native (open bar), saline inhalation (dotted bar), ovalbumin inhalation (closed bar), and ovalbumin inhalation with prednisolone intake mice (oblique bar) after the third inhalation. Six mice each for naive and saline groups and seven mice each for ovalbumin only and ovalbumin and prednisolone groups were analyzed. (D) mRNA expression of IL-13Rα2 was investigated by quantitative RT-PCR analysis, after the first (open bar), the second (dotted bar), or the third (closed bar) of ovalbumin inhalation. Seven mice for each group were analyzed. Statistically significant at $p<0.0001$ (*), or $p<0.005$ (**).

3. Discussion

In this article, we demonstrated that stimulation of IL-4 and IL-13 up-regulated intracellular expression of IL-13Rα2 in human BECs (Figs. 1 and 3) and that the condition inducing bronchial asthma by ovalbumin, in which IL-4 and IL-13 are highly expressed, enhanced expression of IL-13Rα2 in mouse lung tissue (Fig. 7). Expression of IL-13Rα2 on the cell surface of a BEC line inhibited STAT6 activation by IL-13, and IL-13Rα2 was likely to act as a monomeric receptor for IL-13 (Fig. 6), indicating that IL-13Rα2 functions as a decoy receptor in BECs, compatible with recent reports [20,21]. Although both IL-4 and IL-13 induced synthesis of IL-13Rα2 protein, expression of IL-13Rα2 was not detected on the cell surface of human BECs (data not shown). Another factor may be needed for transferring intracellular IL-13Rα2 to the cell surface. It has been reported that IFN-γ has such an action [24]; however, IFN-γ completely inhibited expression of IL-13Rα2 in human BECs (Fig. 1D). Thus far, the precise mechanism of transferring intracellular IL-13Rα2 to the cell surface remains obscure. Our present in vivo findings of high expression of IL-13Rα2 in lung tissues of ovalbumin-induced asthma model mice correspond to the recent reports as of the effects of IL-13 fusion cytotoxin in survived fibroblasts [25] and infection of *Schistosoma mansoni* on liver [26]. Taking these results collectively, it is thought that there would exist a negative-feedback regulation of the IL-13 signal by expression of IL-13Rα2 on the cell surface of human BECs and that this system would act to let the IL-13 signal be self-limited (Fig. 8). The affinities of IL-13Rα2 and the IL-13Rα1/IL-4Rα complex with IL-13 are almost the same [12,27,28]. Furthermore, it was assumed that expression of IL-13Rα2 and the IL-13Rα1/IL-4Rα complex was also at the same level in IL-4/IL-13-stimulating BECs, because mRNA of IL-13Rα2 and IL-4Rα was invariable (Figs. 1 and 2). These data indicate that expressed IL-13Rα2 could physiologically tune the IL-13 signal by competing with the IL-13Rα1/IL-4Rα complex for the IL-13 binding. This regulation is likely to be specific in certain cells such as BECs, because B cells did not up-regulate expression of IL-13Rα2 upon stimulation of anti-IgM Ab/anti-CD40 Ab or IL-4 (data not shown). During the preparation of this article, the analyses of IL-13Rα2-deficient mice have been reported, demonstrating the role of IL-13Rα2 as a down-regulatory factor of the IL-13 signal [26,29].

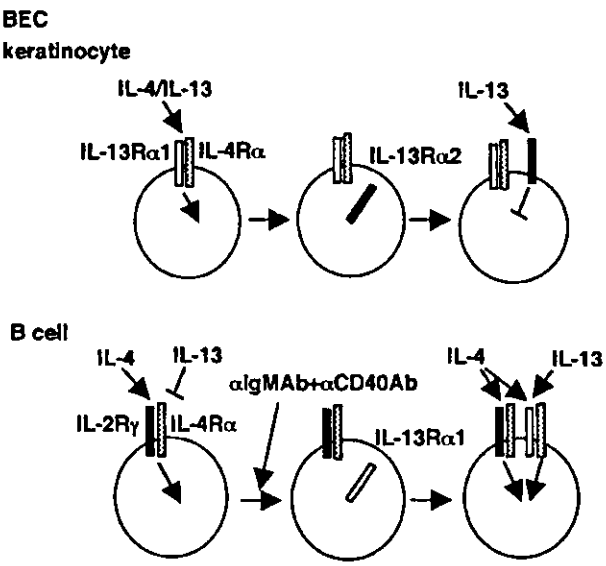

Fig. 8. Schematic model of the regulation of IL-13 receptor expression in BECs and B cells. The IL-13Rα1/IL-4Rα receptor is constitutively expressed on BECs, which can transduce the signal of IL-4/IL-13. The stimulant of IL-4/IL-13 induces expression of IL-13Rα2, which limits the IL-13 signal in these cells. In contrast, the resting stage of B cells express IL-4Rα and IL-2Rγ, not IL-13Rα1, transducing the signal of IL-4, but not of IL-13. Upon activation by anti-IgM Ab and anti-CD40 Ab, B cells express IL-13Rα1, which enables the cells to be responsive to IL-13.

Cytokine signaling is known to have various types of negative-feedback systems, using a ligand, a receptor, or an intracellular signaling molecule to inhibit the signals [30,31]. Some cytokine signaling systems employ a decoy receptor for the negative-feedback system. These are classified into three groups: the Toll/IL-1 receptor family, the TNF receptor family, and the chemokine receptor family [31]. The Toll/IL-1 receptor family includes type II IL-1R and IL-18 binding protein for IL-1 and IL-18, and the TNF receptor family does osteoprotegerin, DcR (decoy receptor)1, DcR2, DcR3 and Fas decoy receptor for RANKL (receptor activator of NF-κB ligand), TRAIL (TNF-α-related apoptosis-inducing ligand), Fas ligand and LIGHT (homologous to lymphotoxins, shows inducible expression, and competes with herpes simplex virus glycoprotein D for herpes virus entry mediator, a receptor expressed by T lymphocytes) [31]. Silent chemokine receptors, DARC (Duffy antigen receptor for chemokines)/Duffy and D6 are thought to act as decoy receptors for several chemokines such as CCL2, CCL5, and CXCL1 [31]. The negative-feedback system by IL-13Rα2 has a unique characteristic, in that ligand itself induces expression of the decoy receptor as IL-1 induces its decoy receptor, type II IL-1R [32]. It may be because persistent IL-13 signal is hazardous for the bronchial tissue, since overexpression of IL-13 in bronchial tissue in mice caused emphysema with enhanced lung volumes and compliance, mucous metaplasia, and inflammation by induction of metalloproteinases and cathepsin proteinases [33].

It remains unknown whether IL-13Rα2 acts as the decoy receptor in a membrane-bound form or a soluble form. There are two possibilities to generate a soluble form of the receptor: alternative splicing and shedding. There exist these two types of production of soluble IL-4Rα [34]. Formation of soluble type II IL-1R is likely to mostly apply shedding by matrix metalloproteinases [31]. Soluble IL-13Rα2 has been detected in the serum and urine of mice [35]. It is of interest to address whether the human counterpart of soluble IL-13Rα2 exists, and if it does, how the soluble type is generated in vivo.

We have shown that IL-13Rα2 induction in human BECs by IL-4 or IL-13 was STAT6-dependent (Fig. 5). IL-4 or IL-13 induces activation of latent STAT6, causing expression of their target genes, which does not require de novo protein synthesis [36]; however, cycloheximide, a protein synthesis inhibitor, blocked expression of IL-13Rα2, but not eotaxin by IL-4 or IL-13 (Fig. 4), indicating that this event is not a direct action of STAT6, but is mediated by an unknown molecule induced by STAT6. Although the molecule that responds to the stimulation of IL-4 or IL-13 and induces expression of IL-13Rα2 remains undetermined, secreted proteins and transcription factors are potent candidates. Microarray analyses by others and us revealed that IL-4 or IL-13 induces various kinds of secreted proteins and transcription factors in human BECs [22,37]. The list of these inducing genes may provide a hint for the clarification of the IL-13Rα2-expression mechanism.

Considering the important roles of IL-13 in the pathogenesis of bronchial asthma based on analyses of model mice, it is reasoned that the imbalance of the IL-13 signal would modulate the susceptibility to or the severity of bronchial asthma. It would involve both genetic and extrinsic factors to up-regulate the signal pathway through the IL-13Rα1/IL-4R complex and down-regulate the binding to IL-13Rα2. As for genetic factors, we recently demonstrated that the variant of *IL13* (Gln^{110}) associated with bronchial asthma [11] showed lower affinity with IL-13Rα2 compared to the wild type (Arg^{110}), although both types possessed the same affinity with the IL-13Rα1/IL-4Rα complex [12]. This means that this variant could relatively enhance the IL-13 signal in bronchial tissues by increasing binding to the IL-13Rα1/IL-4Rα complex. Single nucleotide polymorphisms (SNPs) located on *IL13RA1* and *STAT6* were reported to be associated with atopy or bronchial asthma, although the functional significance of these variants remains undetermined [11,38]. We previously demonstrated that a SNP on *IL4RA* (Ile50Val) is correlated with atopy, up-regulating IgE [39,40]; however, it is still unknown whether this variant also enhances the IL-13 signal. We need to identify other variants among the IL-13 signaling molecules such as IL13RA2, JAK, and the

suppressor of cytokine signal (SOCS) family [13,30]. Extrinsic factors that influence this balance might also be involved in the pathogenesis of bronchial asthma. It has been very recently reported that IL-13Rα2 is expressed on human BECs, although the expression level is variable among normal and asthmatic subjects [41], indicating the heterogeneity of the patients. Further studies aimed at clarifying the expression mechanism of IL-13Rα1, IL-13Rα2, and IL-4Rα, and at identifying the genetic and environmental factors to influence it, would be useful for elucidating the pathogenesis of bronchial asthma.

4. Materials and methods

4.1. Cells and reagents

Human BECs were purchased from Clonetics (Walkersville, MD). The cells were cultured as described before [22]. For stimulation, cells were incubated with the indicated concentrations of human IL-4 or IL-13 (Peprotech, Rocky Hill, NJ) or 10 ng/ml of TNF-α or IFN-γ or 50 ng/ml of IL-1β, IL-5, IL-6, or IL-9 (R&D Systems, Minneapolis, MN) for the indicated period.

A mouse tracheal epithelial cell line, TGMBE-02-3 cells, was kindly given by Basic Technology Research Laboratory, Daiichi Pharmaceutical Co. (Tokyo, Japan) [42]. The cells were cultured in D-MEM/F-12 medium (GIBCO BRL, Rockville, MD) supplemented with 2% FCS, 1% ITES, and 10 ng/ml murine EGF (Wako, Osaka, Japan). For stimulation, cells were incubated with 10 ng/ml of murine IL-4 or 50 ng/ml of murine IL-13 (R&D Systems). In some experiments, the cells were stimulated with either IL-4 or IL-13 in the presence of the indicated concentrations of cycloheximide (Sigma, Saint Louis, MO).

The truncated form of human STAT6 was constructed based on previous reports [43,44]. A PCR amplification from plasmid including the full coding sequence of STAT6 cDNA (kindly given by Dr. G. Honda, Asahi Kasei Co., Fuji, Japan) was performed with primer pairs (5′-TTGGTACCATGTCTCTGTGGGGTC-3′, and 5′-GCGGCCGCCTACTGGAGCTCTGGGGTAGGAAGTG-3′) using Expand High Fidelty PCR System (Roche Diagnostics, Tokyo, Japan), leading to generation of cDNA encoding the truncated form of STAT6 (1–662 amino acids). The product was first digested with *Kpn*I, and this site was blunt-ended by Blunting High (TOYOBO, Osaka, Japan), then cleaved by *Not*I. The fragment was cloned into pIRESneo2 (Clontech, Palo Alto, CA) by *Stu*I (blunt) and *Not*I. This construct was transfected into TGMBE-02-3 cells by TransFast™ Transfection Reagent (Promega, Madison, WI), and the transfectants were maintained with a medium containing 200 μg/ml of Geneticin (Sigma).

The transformed human BEC line, BEAS-2B was purchased from ATCC (CRL-9609). Cells were cultured with F-12 nutrient mixture (Ham's F-12, GIBCO BRL) containing 10% FCS. The plasmid including IL-13Rα2 and a neomycin-resistant gene in pME18S mammalian expression vector [12] was transfected into BEAS-2B cells by TransFast™ Transfection Reagent. Expression of IL-13Rα2 was confirmed by flow cytometry using anti-IL-13Rα2 Ab (B-D13; Diaclone, Besançon, France). The transfectants were maintained with a medium containing 500 μg/ml of Geneticin.

4.2. Quantitative RT-PCR analysis

Quantitative analysis of mRNA expression was performed using the ABI PRISM™ 7700 sequence detection system (Applied Biosystems Japan, Tokyo, Japan) as described before [22]. The primers and TaqMan™ probes used for the analyses were designed according to the manufacturer's software, Primer Express (Applied Biosystems Japan, Table 1). To calculate the copy numbers for each gene, a standard curve was drawn using a plasmid containing a PCR amplified sequence whose copy number was known. To normalize the cDNA concentration in each sample, the copy number of GAPDH was quantified.

4.3. Immunocytochemical analysis

After HBECs were fixed for 10 min by 100% cold ethanol, air-dried and then processed by the standard methods, they were incubated with either an mAb against anti-IL-13Rα1 (UU15 [11,18]) or against anti-IL-13Rα2 (B-D13) for 1 h at room temperature. The antigen was detected by the avidin–biotin complex immunoperioxidase (ABC) method, as previously described [45]. As a negative control, PBS or normal mouse IgG was used instead of each primary antibody.

4.4. RT-PCR

Total RNA was extracted from TGMBE-02-3 cells by ISOGEN (Nippongene, Tokyo, Japan). The RT reaction primed with random hexamer was performed using GeneAmp RNA PCR Kit (Applied Biosystems Japan), according to the manufacturer's instruction. The PCR reaction was performed with cDNA as a template using the primers given below after an initial 1 min denaturation at 96 °C, followed by 40 cycles of 96 °C for 1 min, either 51 °C for 1 min for IL-13Rα2 and GAPDH or 60 °C for 1 min for eotaxin, and 72 °C for 1 min. The PCR primers used were 5′-TGCTCAGATGACGGAATTTGG-3′, and 5′-TGGTAGCCAGAAACGTAGCAAAG-3′ for IL-13Rα2, 5′-CCCAACTTCCTGCTGCTTTATCATG-3′ and 5′-AGCCAAGTCCTTGGGCGACTGGT-3′ for

Table 1
Primers used for the quantitative PCR analysis

	Forward	Reverse	TaqMan™ probe
Human IL-13Rα1	5′-CCAATGAGAGTGAGAAGCCTAGC-3′	5′-TGCATTGAAGCTCAGTCACAGC-3′	5′-AAAATGCATCACCCCCAGAAGGTGATC-3′
Human IL-13Rα2	5′-TGCTCAGATGACGGAAATTTGG-3′	5′-TGGTAGCCAGAAACGTAGCAAAG-3′	5′-TGAGTGGAGTGATAAACAATGCTGGGAAGG-3′
Human IL-4Rα	5′-AATGGTCCCACCAATTGCA-3′	5′-GCGCCTCCGTTGTTCTCA-3′	5′-AGCTGGTTTTTCTGCTCTCCGAAGCC-3′
Mouse IL-13Rα1	5′-GATTGGAGTGAAGCACAGAGTATAGG-3′	5′-GGATTATGACTGCCACTGCGA-3′	5′-AGGAGCAAAACTCCACCTTCTACACCACCA-3′
Mouse IL-13Rα2	5′-ACACAGGGCCAGACTCAAAGAT-3′	5′-GCACACACTTCTTTGTTCAGATCC-3′	5′-AACCTGAACCCACATTGAGCCTCCATG-3′
Mouse IL-4Rα	5′-CACTACAGGCTGATGTTCTTCGA-3′	5′-TGGACCGGCCTATTCATTTC-3′	5′-ACCTCACATGCATCCCGAGGAACAGT-3′

eotaxin, and 5′-GCACCACCAACTGCTTAGCC-3′ and 5′-CTTTGGCATTGTGGAAGGGCTCATG-3′ for GAPDH.

4.5. Electrophoretic mobility shift assay (EMSA)

Procedures of EMSA were carried out as described before [46]. Nuclear extract was mixed with binding buffer (20 mM Hepes–NaOH, pH 7.9, 2 mM EDTA, 100 mM NaCl, 10% glycerol, 0.2% Nonidet P-40), poly(dI-dC), and ^{32}P-labeled double-stranded oligonucleotide probe (5′-GTCAACTTCCCAAGAACAGAA-3′). The mixtures were incubated at room temperature for 30 min. The reaction mixtures were loaded on a 4% polyacrylamide gel.

4.6. Western blotting analysis

Western blotting was conducted as previously described [16]. Mock-transfected or IL-13Rα2-transfected BEAS-2B cells were incubated in the absence or presence of 10 ng/ml of IL-4 or 50 ng/ml of IL-13 for 10 min at 37 °C. Cell lysates were applied to SDS-PAGE and transferred electrophoretically to a PVDF membrane (Amersham, Arlington Heights, IL). Proteins were probed with anti-phospho STAT6 Ab (New England Biolabs, Beverly, MA) or anti-STAT6 Ab (Santa Cruz Biotechnology, Santa Cruz, CA).

4.7. Cross-linking of ^{125}I-IL-13

Radiolabeling of IL-13 and chemical cross-linking were performed as described before [47]. The concentration of the labeled IL-13 was determined by self-displacement binding to the IL-13Rα2-expressing BEAS-2B cells with non-radiolabeled IL-13 at a known concentration. After cells were incubated with 150 pM of ^{125}I-labeled IL-13 for 2 h at 4 °C in the presence or absence of cold IL-13, a cross-linker (BS^3; Pierce, Rockford, IL) was added, and then cells were washed. Cell lysates were subjected to SDS-PAGE and autoradiography.

4.8. Generation of asthma model mice

Generation of asthma model mice was performed as described before [23]. Seven-week-old male BALB/c mice were used for this experiment. Mice were actively sensitized by intraperitoneal injections of 50 μg ovalbumin (Seikagaku Kogyo, Tokyo, Japan) with 1 mg alum on day 0 and day 12. Starting on day 22, they were exposed to inhalation of 1% ovalbumin or saline for 30 min, three times every fourth day. The aerosol was generated by a nebulizer (Ultrasonic nebulizer UN-701, Azwell Co. Ltd., Osaka, Japan) driven by filling a perspex cylinder chamber with a nebulized solution. In the prednisolone

group, 5 mg/kg of prednisolone (Shionogi & Co. Ltd, Osaka, Japan) was given orally every day from day 22. Mouse lungs were removed for mRNA preparation after the third inhalation under anesthesia with sodium pentobarbitone (100 mg/kg, i.p.). In some experiments, mouse lungs were removed from the first or second inhalation. The procedures were conducted according to the 'Guide for the Care and Use of Laboratory Animals', and the study was approved by Gifu Pharmaceutical University's Animal Committee.

Acknowledgements

We thank Dr. Dovie R. Wylie for critical review of this manuscript. We also thank Drs. Toshihiko Akimoto and Norifumi Sugiyama for providing TGMBE-02-3 cells, and Dr. Goichi Honda for providing the plasmid encoding STAT6. This work was supported in part by a Research Grant for Immunology, Allergy and Organ Transplant from the Ministry of Health and Welfare of Japan, a grant-in-aid for Scientific Research from the Ministry of Education, Science, Sports and Culture of Japan.

References

[1] Holgate ST. The epidemic of allergy and asthma. Nature 1999;402:B2–4.
[2] Akimoto T, Numata F, Tamura M, Takata Y, Higashida N, Takashi T, et al. Abrogation of bronchial eosinophilic inflammation and airway hyperreactivity in signal transducers and activators of transcription (STAT)6-deficient mice. J Exp Med 1998;187:1537–42.
[3] Cohn L, Homer RJ, MacLeod H, Mohrs M, Brombacher F, Bottomly K. Th2-induced airway mucus production is dependent on IL-4Rα, but not on eosinophils. J Immunol 1999;162:6178–83.
[4] Webb DC, McKenzie AN, Koskinen AM, Yang M, Mattes J, Foster PS. Integrated signals between IL-13, IL-4, and IL-5 regulate airways hyperreactivity. J Immunol 2000;165:108–13.
[5] Wills-Karp M, Luyimbazi J, Xu X, Schofield B, Neben TY, Karp CL, et al. Interleukin-13: central mediator of allergic asthma. Science 1998;282:2258–61.
[6] Grünig G, Warnock M, Wakil AE, Venkayya R, Brombacher F, Rennick DM, et al. Requirement for IL-13 independently of IL-4 in experimental asthma. Science 1998;282:2261–3.
[7] Zhu Z, Homer RJ, Wang Z, Chen Q, Geba GP, Wang J, et al. Pulmonary expression of interleukin-13 causes inflammation, mucus hypersecretion, subepithelial fibrosis, physiologic abnormalities, and eotaxin production. J Clin Invest 1999;103:779–88.
[8] Kuperman DA, Huang X, Koth LL, Chang GH, Dolganov GM, Zhu Z, et al. Direct effects of interleukin-13 on epithelial cells cause airway hyperreactivity and mucus overproduction in asthma. Nat Med 2002;8:885–9.
[9] Kotsimbos TC, Ernst P, Hamid QA. Interleukin-13 and interleukin-4 are coexpressed in atopic asthma. Proc Assoc Am Physicians 1996;108:368–73.
[10] Bodey KJ, Semper AE, Redington AE, Madden J, Teran LM, Holgate ST, et al. Cytokine profiles of BAL T cells and T-cell clones obtained from human asthmatic airways after local allergen challenge. Allergy 1999;54:1083–93.
[11] Heinzmann A, Mao XQ, Akaiwa M, Kreomer RT, Gao PS, Ohshima K, et al. Genetic variants of IL-13 signalling and human asthma and atopy. Hum Mol Genet 2000;9:549–59.
[12] Arima K, Umeshita-Suyama R, Sakata Y, Akaiwa M, Mao XQ, Enomoto T, et al. Upregulation of IL-13 concentration *in vivo* by the *IL13* variant associated with bronchial asthma. J Allergy Clin Immunol 2002;109:980–7.
[13] Izuhara K, Umeshita-Suyama R, Akaiwa M, Shirakawa T, Deichmann KA, Arima K, et al. Recent advances in understanding how interleukin-13 signals are involved in the pathogenesis of bronchial asthma. Arch Immunol Ther Exp 2000;48:505–12.
[14] Izuhara K, Arima K, Yasunaga S. IL-4 and IL-13: their pathological roles in allergic diseases and their potential in developing new therapies. Curr Drug Targets Inflamm Allergy 2002;1:263–9.
[15] Orchansky PL, Kwan R, Lee F, Schrader JW. Characterization of the cytoplasmic domain of interleukin-13 receptor-α. J Biol Chem 1999;274:20818–25.
[16] Umeshita-Suyama R, Sugimoto R, Akaiwa M, Arima K, Yu B, Wada M, et al. Characterization of IL-4 and IL-13 signals dependent on the human IL-13 receptor α chain 1: redundancy of requirement of tyrosine residue for STAT3 activation. Int Immunol 2000;12:1499–509.
[17] Ogata H, Ford D, Kouttab N, King TC, Vita N, Minty A, et al. Regulation of interleukin-13 receptor constituents on mature human B lymphocytes. J Biol Chem 1998;273:9864–71.
[18] Akaiwa M, Yu B, Umeshita-Suyama R, Terada N, Suto H, Koga T, et al. Localization of human interleukin 13 receptor in non-haematopoietic cells. Cytokine 2001;13:75–84.
[19] Ihle JN, Witthuhn BA, Quelle FW, Yamamoto K, Silvennoinen O. Signaling through the hematopoietic cytokine receptors. Annu Rev Immunol 1995;13:369–98.
[20] Kawakami K, Taguchi J, Murata T, Puri RK. The interleukin-13 receptor α2 chain: an essential component for binding and internalization but not for interleukin-13-induced signal transduction through the STAT6 pathway. Blood 2001;97:2673–9.
[21] Bernard J, Treton D, Vermot-Desroches C, Boden C, Horellou P, Angevin E, et al. Expression of interleukin 13 receptor in glioma and renal cell carcinoma: IL13Rα2 as a decoy receptor for IL13. Lab Invest 2001;81:1223–31.
[22] Yuyama N, Davies DE, Akaiwa M, Matsui K, Hamasaki Y, Suminami Y, et al. Analysis of novel disease-related genes in bronchial asthma. Cytokine 2002;19:287–96.
[23] Tanaka H, Kawada N, Yamada T, Kawada K, Takatsu K, Nagai H. Allergen-induced airway inflammation and bronchial responsiveness in interleukin-5 receptor α chain-deficient mice. Clin Exp Allergy 2000;30:874–81.
[24] Daines MO, Hershey GK. A novel mechanism by which interferon-gamma can regulate interleukin (IL)-13 responses. Evidence for intracellular stores of IL-13 receptor α-2 and their rapid mobilization by interferon-γ. J Biol Chem 2002;277:10387–93.
[25] Jakubzick C, Kunkel SL, Joshi BH, Puri RK, Hogaboam CM. Interleukin-13 fusion cytotoxin arrests *Schistosoma mansoni* egg-induced pulmonary granuloma formation in mice. Am J Pathol 2002;161:1283–97.
[26] Chiaramonte MG, Mentink-Kane M, Jacobson BA, Cheever AW, Whitters MJ, Goad ME, et al. Regulation and function of the interleukin 13 receptor α 2 during a T helper cell type 2-dominant immune response. J Exp Med 2003;197:687–701.
[27] Aman MJ, Tayebi N, Obiri NI, Puri RK, Modi WS, Leonard WJ. cDNA cloning and characterization of the human interleukin 13 receptor α chain. J Biol Chem 1996;271:29265–70.
[28] Caput D, Laurent P, Kaghad M, Lelias J-M, Lefort S, Vita N, et al. Cloning and characterization of a specific interleukin (IL)-13 binding protein structurally related to the IL-5 receptor α chain. J Biol Chem 1996;271:16921–6.

[29] Wood N, Whitters MJ, Jacobson BA, Witek J, Sypek JP, Kasaian M, et al. Enhanced interleukin (IL)-13 responses in mice lacking IL-13 receptor α 2. J Exp Med 2003;197:703–9.
[30] Yasukawa H, Sasaki A, Yoshimura A. Negative regulation of cytokine signaling pathways. Annu Rev Immunol 2000;18: 143–64.
[31] Mantovani A, Locati M, Vecchi A, Sozzani S, Allavena P. Decoy receptors: a strategy to regulate inflammatory cytokines and chemokines. Trends Immunol 2001;22:328–36.
[32] Colotta F, Re F, Muzio M, Bertini R, Polentarutti N, Sironi M, et al. Interleukin-1 type II receptor: a decoy target for IL-1 that is regulated by IL-4. Science 1993;261:472–5.
[33] Zheng T, Zhu Z, Wang Z, Homer RJ, Ma B, Riese RJ, et al. Inducible targeting of IL-13 to the adult lung causes matrix metalloproteinase- and cathepsin-dependent emphysema. J Clin Invest 2000;106:1081–93.
[34] Blum H, Wolf M, Enssle K, Röllinghoff M, Gessner A. Two distinct stimulus-dependent pathways lead to production of soluble murine interleukin-4 receptor. J Immunol 1996;157: 1846–53.
[35] Zhang JG, Hilton DJ, Willson TA, McFarlane C, Roberts BA, Moritz RL, et al. Identification, purification, and characterization of a soluble interleukin (IL)-13-binding protein. Evidence that it is distinct from the cloned IL-13 receptor and IL-4 receptor α-chains. J Biol Chem 1997;272:9474–80.
[36] Schindler C, Darnell JE Jr. Transcriptional responses to polypeptide ligands: the JAK-STAT pathway. Annu Rev Biochem 1995;64:621–51.
[37] Lee JH, Kaminski N, Dolganov G, Grunig G, Koth L, Solomon C, et al. Interleukin-13 induces dramatically different transcriptional programs in three human airway cell types. Am J Respir Cell Mol Biol 2001;25:474–85.
[38] Gao P-S, Mao X-Q, Arinobu Y, Izuhara K, Roberts MH, Deichmann KA, et al. Stat6 and atopic asthma. J Med Genet 2000;37:380–2.
[39] Mitsuyasu H, Izuhara K, Mao X-Q, Gao P-S, Arinobu Y, Enomoto T, et al. Ile50Val variant of IL4Rα upregulates IgE synthesis and associates with atopic asthma. Nat Genet 1998; 19:119–20.
[40] Mitsuyasu H, Yanagihara Y, Mao X-Q, Gao P-S, Arinobu Y, Ihara K, et al. Dominant effect of Ile50Val variant of the human interleukin-4 receptor α chain in IgE synthesis. J Immunol 1999;162:1227–31.
[41] Lordan JL, Bucchieri F, Richter A, Konstantinidis A, Holloway JW, Thornber M, et al. Cooperative effects of Th2 cytokines and allergen on normal and asthmatic bronchial epithelial cells. J Immunol 2002;169:407–14.
[42] Sugiyama N, Tabuchi Y, Numata F, Uchida Y, Horiuchi T, Ishibashi K, et al. Establishment and characterization of tracheal epithelial cell lines, TM01 and TM02-3, from transgenic mice bearing temperature-sensitive simian virus 40 large T-antigen gene. Cell Struct Funct 1998;23:119–27.
[43] Mikita T, Campbell D, Wu P, Williamson K, Schindler U. Requirements for interleukin-4-induced gene expression and functional characterization of Stat6. Mol Cell Biol 1996;16: 5811–20.
[44] Masuda A, Matsuguchi T, Yamaki K, Hayakawa T, Kubo M, LaRochelle WJ, et al. Interleukin-15 induces rapid tyrosine phosphorylation of STAT6 and the expression of interleukin-4 in mouse mast cells. J Biol Chem 2000;275:29331–7.
[45] Toda S, Matsumura S, Fujitani N, Nishimura T, Yonemitsu N, Sugihara H. Transforming growth factor-β1 induces a mesenchyme-like cell shape without epithelial polarization in thyrocytes and inhibits thyroid folliculogenesis in collagen gel culture. Endocrinology 1997;138:5561–75.
[46] Izuhara K, Heike T, Otsuka T, Yamaoka K, Mayumi M, Imamura T, et al. Signal transduction pathway of interleukin-4 and interleukin-13 in human B cells derived from X-linked severe combined immunodeficiency patients. J Biol Chem 1996;271: 619–22.
[47] Izuhara K, Miyajima A, Harada N. The chimeric receptor between interleukin-2 receptor β chain and interleukin-4 receptor transduces interleukin-2 signal. Biochem Biophys Res Commun 1993;190:992–1000.

THE JOURNAL OF BIOLOGICAL CHEMISTRY

Vol. 278, No. 46, Issue of November 14, pp. 45296–45304, 2003
Printed in U.S.A.

Inhibitory Mechanism of a Cross-class Serpin, the Squamous Cell Carcinoma Antigen 1*

Received for publication, July 17, 2003, and in revised form, August 29, 2003
Published, JBC Papers in Press, August 29, 2003, DOI 10.1074/jbc.M307741200

Kiyonari Masumoto‡, Yasuhisa Sakata‡, Kazuhiko Arima‡, Isao Nakao‡, and Kenji Izuhara‡§¶

From the ‡Division of Medical Biochemistry, Department of Biomolecular Sciences and the §Division of Medical Research, Center for Comprehensive Community Medicine, Saga Medical School, 5-1-1, Nabeshima, Saga, 849-8501, Japan

The squamous cell carcinoma antigen (SCCA) 1 and its homologous molecule, SCCA2, belong to the ovalbumin-serpin family. Although SCCA2 inhibits serine proteinases such as cathepsin G and mast cell chymase, SCCA1 targets cysteine proteinases such as cathepsin S, K, L, and papain. SCCA1 is therefore called a cross-class serpin. The inhibitory mechanism of the standard serpins is well characterized; those use a suicide substrate-like inhibitory mechanism during which an acyl-enzyme intermediate by a covalent bond is formed, and this complex is stable against hydrolysis. However, the inhibitory mechanism of cross-class serpins remains unresolved. In this article, we analyzed the inhibitory mechanism of SCCA1 on a cysteine proteinase, papain. SCCA1 interacted with papain at its reactive site loop, which was then cleaved, as the standard serpins. However, gel-filtration analyses showed that SCCA1 did not form a covalent complex with papain, in contrast to other serpins. Interaction with SCCA1 severely impaired the proteinase activity of papain, probably by inducing conformational change. The decreased, but still existing, proteinase activity of papain was completely inhibited by SCCA1 according to the suicide substrate-like inhibitory mechanism; however, papain recovered its proteinase activity with the compromised level, when all of intact SCCA1 was cleaved. These results suggest that the inhibitory mechanism of SCCA1 is unique among the serpin superfamily in that SCCA1 performs its inhibitory activity in two ways, contributing the suicide substrate-like mechanism without formation of a covalent complex and causing irreversible impairment of the catalytic activity of a proteinase.

The serpins (serine proteinase inhibitors) are a superfamily of proteinase inhibitors characterized by a conserved structure and employing a suicide substrate-like inhibitory mechanism (1, 2). The structure of the serpins consists of three β sheets (A—C), nine α helices (A–I), and the reactive site loop (RSL)[1] composed of ~17 amino residues (1). The inhibitory mechanism of the serpin is well characterized (2). The exposed RSL of the serpin is recognized by the proteinase, and an initial non-covalent Michaelis encounter complex is formed. Then, in the inhibitory pathway, a "bait" peptide bond (P1-P1′) that mimics the normal substrate of the proteinase is attacked by the active serine residue of the proteinase, subsequently forming an acyl-enzyme intermediate linked by an oxy-ester bond. In the cleaved form, the P side of the RSL inserts into the body of the protein, which dramatically changes the conformations of the serpin and the proteinase, making it impossible for the ester bond to hydrolyze (3). In the non-inhibitory or substrate pathways, the serpin is cleaved by the proteinase just as the substrate of the proteinase after the Michaelis encounter complex is formed. It has been revealed that the serpins are involved in various kinds of biological functions: fibrinolysis, coagulation, inflammation, tumor cell invasion, cellular differentiation, and apoptosis (1).

The squamous cell carcinoma antigen (SCCA) 1 (SERPINB3) and SCCA2 (SEPINB4) belong to the ovalbumin-serpin family, and these proteins are 91% identical at the amino acid level (4). Both genes locate at 18q21.3 very closely, generating a cluster of serpins together with plasminogen activator inhibitor type 2 and maspin, suggesting that either the *SERPINB3* or the *SEPINB4* gene could arise from the other by gene duplication (5). SCCA1 was originally purified from squamous cell carcinoma of uterine cervix (6), and it turned out later that SCCA1 and SCCA2 were co-expressed broadly in normal tissues: the epithelium of tongue, tonsil, esophagus, uterine cervix, vagina, and the conducting airways; Hassall's corpuscles of the thymus; and some areas of the skin (7). The biological functions of SCCA1 and SCCA2 still remain obscure. It has been reported that these proteins confer resistance against tumor necrosis factor-α- or radiation-inducing apoptosis (8–10). We have recently shown that expression of both SCCA1 and SCCA2 is up-regulated by two related Th2-type cytokines, IL-4 and IL-13, in bronchial epithelial cells and that SCCA expression is also augmented in bronchial lesions and in peripheral blood of bronchial asthma patients (11). These results shed light on the probable novel pathophysiological roles of SCCA1 and SCCA2.

Although SCCA1 and SCCA2 are very homologous, SCCA1 has unique properties as a serpin; SCCA1 inhibits cysteine proteinases such as cathepsin K, L, S, and papain, whereas SCCA2 inhibits serine proteinases such as cathepsin G and human mast cell chymase (HMC) (4, 12, 13). Although target proteinases for most serpins are the chymotrypsin family, very few serpins inhibit cysteine proteinases: for example, cytokine response modifier A (CrmA) produced by cowpox virus and proteinase inhibitor 9 (PI9, SERPINB9) are known to inhibit caspase proteins (cysteine proteinases) (14–16). Such a proteinase inhibitor is defined as a cross-class inhibitor, and thus far, CrmA, PI9, and SCCA1 are all obvious cross-class serpins

* This work was supported in part by a research grant for immunology, allergy and organ transplant from the Ministry of Health, Welfare, and Labor of Japan and a grant-in-aid for scientific research from the Japan Society for the Promotion of Science. The costs of publication of this article were defrayed in part by the payment of page charges. This article must therefore be hereby marked "*advertisement*" in accordance with 18 U.S.C. Section 1734 solely to indicate this fact.

¶ To whom correspondence should be addressed. Tel.: 81-952-34-2261; Fax: 81-952-34-2058; E-mail: kizuhara@med.saga-u.ac.jp.

[1] The abbreviations used are: RSL, reactive site loop; SCCA, squamous cell carcinoma antigen; HMC, human mast cell chymase; CrmA, cytokine response modifier A; PI9, proteinase inhibitor 9; GST, glutathione *S*-transferase; Ab, antibody; MALDI-TOF, matrix-associated laser desorption ionization time-of-flight; BS^3, bis(sulfosuccinimididyl)-suberate; MCA, methylcoumarin ; Suc, succinyl; Z, benzyloxycarbonyl; Bz-Arg-MCA, benzoyl-Arg-7-amino-4-methylcoumarin.

(1). The specificities of SCCA1 and SCCA2 are due to a difference in the RSL sequences because only 7 amino acid residues among 13 (54%) were identical in the RSL regions (P7 to P6') of these proteins (17). SCCA2 employs the typical suicide substrate-like inhibitory mechanism of the serpins. Through this mechanism, SCCA2 and serine proteinases are linked by the covalent oxy-ester bond, which is SDS-resistant (4). In contrast, the inhibitory mechanism of cross-class serpins, including SCCA1 on cysteine proteinases, remains unclear. It has been reported that SCCA1 and cathepsin S form an SDS-resistant complex, although its amount is very small (13). Other cross-class serpins, CrmA and PI9, do not form SDS-resistant complexes with caspase proteins, although they do so with a serine proteinase, granzyme B (14, 16, 18, 19). It has not yet been answered how cysteine proteinases lose their catalytic activities, although the thiol-ester bonds between the cross-class serpins and cysteine proteinases are unstable.

In this article, we analyze the inhibitory mechanism of SCCA1 on papain. To retain the native association between SCCA1 and papain, we used gel-filtration system analyses. It turned out that the association between SCCA1 and papain was non-covalent and that the interaction with SCCA1 severely impaired the proteinase activity of papain. These results indicated the unique inhibitory mechanism of SCCA1 among the serpin superfamily.

EXPERIMENTAL PROCEDURES

Materials—Papain, glucose 6-phosphate dehydrogenase, and chicken ovalbumin were purchased from Sigma. E-64, cathepsin G, cathepsin L, HMC, blue dextran 2000, porcine thyroglobulin, ferritin, and bovine serum albumin were purchased from Peptide Institute Inc. (Osaka, Japan), Calbiochem, Athens Research & Technology (Athens, GA), Cortex Biochem (San Leandro, CA), Amersham Biosciences, SERVA Electrophoresis GmbH (Heidelberg, Germany), Roche Applied Science, and Wako (Osaka, Japan), respectively.

Generation of the SCCA1 and SCCA2 Protein—*SERPINB3* and *SERPINB4* cDNA, prepared as reported before (9), were incorporated into pGEX(-KG)-4T (Amersham Biosciences). SCCA2 mutants were generated by PCR-based site-directed mutagenesis, using two complementary primers (Proligo Japan, Kyoto, Japan), designed to introduce a single codon mutation by substituting for the corresponding SCCA1 residue at the RSL. Standard PCR amplification was performed using the SCCA2 cDNA as a template and a mixture of primers. Resulting amplified fragments were treated with *DpnI* (New England Biolabs, Beverly, MA). Isolated plasmid DNAs were digested with *StuI*/*XbaI* and then ligated into the *StuI*/*XbaI* site of the pGEX-KG-SCCA2 plasmid. The RSL replacement mutants of SCCA1 and SCCA2 were similarly generated by digestion and ligation into their *StuI*/*XbaI* site.

Glutathione S transferase (GST)-fused SCCA1 and SCCA2 proteins were expressed in an *Escherichia coli* strain, BL21, and isolated by using glutathione-Sepharose 4B beads (Amersham Biosciences). Purity of the generated proteins was greater than 95% as estimated by SYPRO Ruby staining (Molecular Probes, Eugene, OR). Concentrations of the proteins were determined by Protein Assay (Bio-Rad).

Enzyme Assays—The substrates used for enzyme assays of papain and cathepsin L were benzoyl-Arg-7-amino-4-methylcoumarin (Bz-Arg-MCA) and benzyloxycarbonyl-Phe-Arg-methylcoumarin (Z-FR-MCA), respectively, and succinyl-Ala-Ala-Pro-Phe-methylcoumarin (Suc-AAPF-MCA) was used for cathepsin G and HMC, all purchased from Peptide Institute Inc. The molar concentrations of papain were determined by active site titration with E-64. The indicated concentration of each enzyme was incubated with indicated concentrations of GST-fused SCCA1 or SCCA2 for 30 min at 25 °C in activity-measuring buffer. The buffer was composed of 50 mM sodium acetate (pH 5.5), 4 mM dithiothreitol, 1 mM EDTA, and 1% bovine serum albumin for papain, or 50 mM sodium acetate (pH 5.5), 4 mM dithiothreitol, 1 mM EDTA, and 0.001% bovine serum albumin for cathepsin L, or phosphate-buffered saline containing 0.001% bovine serum albumin for cathepsin G and HMC as described previously (4). Upon addition of the substrate to the reaction mixture, the residual enzyme activity was measured by continuous monitoring using excitation and emission wavelengths of 380 and 460 nm, respectively.

Separation of the Incubated SCCA1 and Papain—After the indicated concentrations of papain and 54 μM GST-fused SCCA1 were incubated in the acetate reaction buffer for 30 min at 25 °C, the reaction mixture was applied to a high pressure-liquid chromatography system equipped with ProteinPak 300SW (Waters, Milford, MA). Then, the subjected samples were eluted with the acetate buffer (50 mM sodium acetate; pH 5.5), and each fraction was subjected to SDS-PAGE or the enzyme assay. The amounts of the proteins on the gels were estimated by protein assay.

Western Blotting—The samples were applied to SDS-PAGE and then electrophoretically transferred to polyvinylidene difluoride membranes (Amersham Biosciences). The membranes were blotted by either anti-papain polyclonal antibody (Ab) (Rockland, Gilbertsville, PA) or anti-GST monoclonal Ab (Upstate Biotechnology, Lake Placid, NY). The proteins were visualized by enhanced chemiluminescence (ECL, Amersham Biosciences).

Amino Acid Sequencing Analysis—The reaction mixture was applied to SDS-PAGE followed by staining with Coomassie Blue R250 in 50% methanol, and then transferred to polyvinylidene difluoride membranes (Bio-Rad). Amino acid sequence analysis of the transferred peptides was performed using an Applied Biosystems 477A/120A protein sequencer (ABI Applied Biosystems, Foster City, CA).

Matrix-associated Laser Desorption Ionization Time-of-Flight (MALDI-TOF) Mass Spectrometry—Papain (4.5 μM) and 36 μM GST-fused SCCA1 were mixed in the acetate reaction buffer for 30 min at 25 °C, and 18 μM E-64 was added to stop the reaction. Then, the reactive samples were applied to Voyager RP MALDI-TOF mass spectrometry (PerSeptive Biosystems, Framingham, MA).

Chemical Cross-linking of Papain and SCCA1—Fifty-five μM GST-fused SCCA1 and 12 μM papain were incubated in the acetate reaction buffer for 5 min at 25 °C followed by incubation with 20 μM bis(sulfosuccinimidyl)suberate (BS^3, Pierce) for 30 min at 25 °C. The reacted samples were applied to SDS-PAGE.

Chemical Modification of the Cysteine Residues of Papain—Eluted papain (0.4 μM) was incubated with 77 μM EZ-Link PEO-maleimide activated biotin {(+)-biotinyl-3-maleimidopropionamidyl-3, 6-dioxaoctanediamine} (PEO-M-biotin, Pierce) for 2 h at 25 °C. The samples were applied to SDS-PAGE and then transferred to polyvinylidene difluoride membranes. The membranes were blotted with horseradish peroxidase-conjugated streptavidin (Zymed Laboratories Inc., South San Francisco, CA).

RESULTS

Expression and Purification of Functional SCCA1 and SCCA2—To perform functional analyses of SCCA1 and SCCA2, we expressed and purified recombinant proteins of GST-fused SCCA1 and SCCA2. Purity of these two proteins was more than 95%, as estimated by SYPRO Ruby staining (Fig. 1*A*). We first confirmed proteinase-inhibitory effects of these two proteins. We examined the inhibitory effects of SCCA1 and SCCA2 on papain, cathepsin L, cathepsin G, and HMC. The K_m and k_{cat} values of papain used in the experiments were estimated as 23.8 ± 2.29 μM and 7.95 ± 0.218 s^{-1} (mean ± S.D., $n = 3$), respectively, which were compatible with those reported in the literature (20). SCCA1 inhibited cysteine proteinase activities of papain and cathepsin L but not the serine proteinase activities of cathepsin G and HMC, whereas SCCA2 showed the opposite effects (Fig. 1*B*), as reported previously (4, 13). SCCA1 inhibited the catalytic activity of papain in a dose-dependent manner, and the stoichiometry of inhibition value was estimated as 4.6 ± 0.1 at 10 nM SCCA1 ($n = 3$, Fig. 1*B*).

It has been demonstrated that SCCA2 and cathepsin G form an SDS-resistant complex by a covalent bond (4). We next analyzed how SCCA1 generated a complex with papain similar to that done by SCCA2 with cathepsin G. SCCA2 formed an SDS-resistant complex with cathepsin G but not with papain, whereas SCCA1 did not show any formation of a complex with either papain or cathepsin G (Fig. 1*C*). These results raised a possibility that SCCA1 performs its proteinase-inhibitory activity without generation of a covalent bond.

Non-covalent Bond of SCCA1 and Papain—Although an SDS-resistant complex between SCCA1 and papain was not detected, it would be possible that the covalent bond between

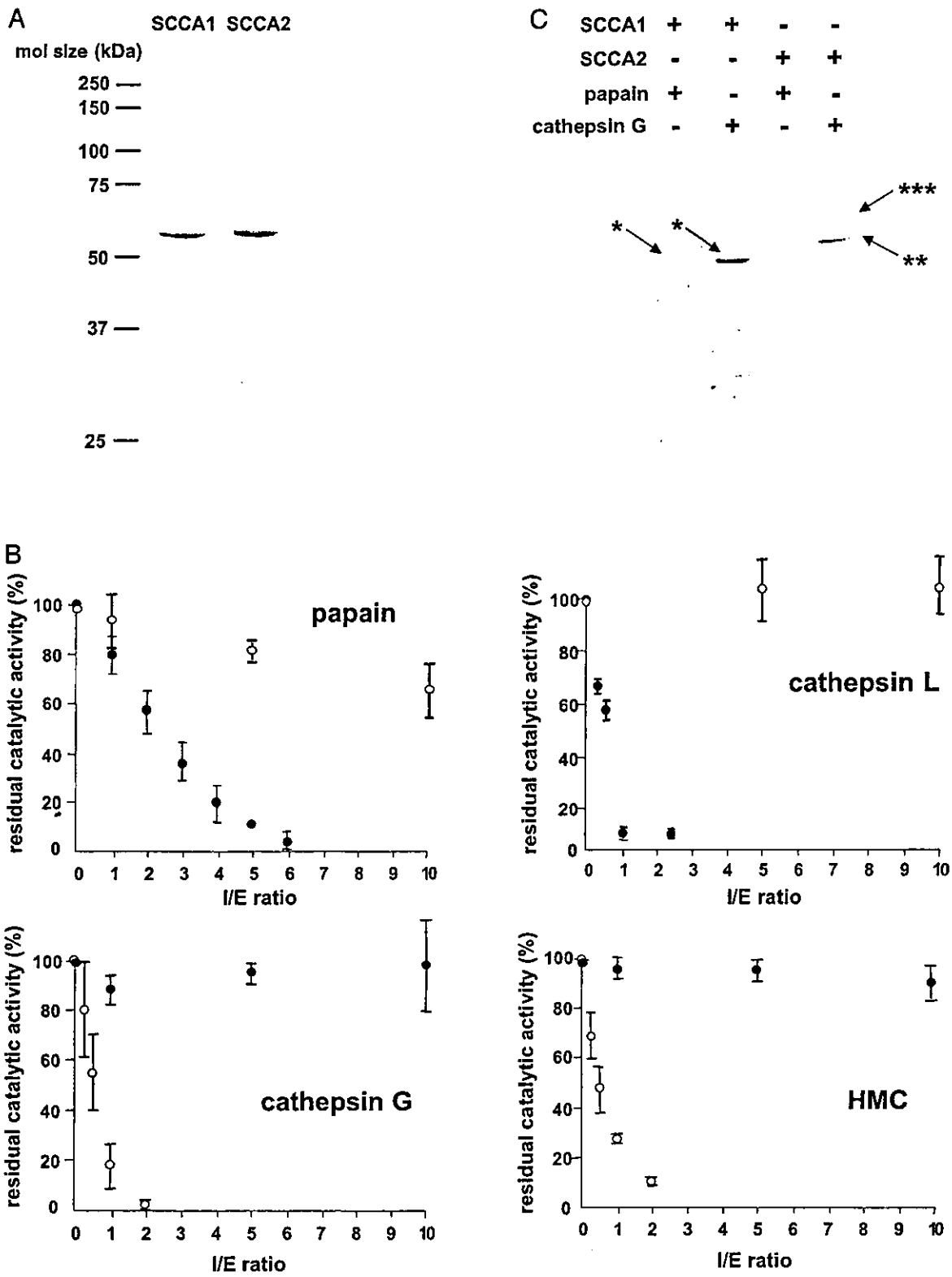

FIG. 1. **Expression and function of SCCA1 and SCCA2.** In *A*, purified recombinant proteins of GST-fused SCCA1 and SCCA2 stained by SYPRO Ruby are depicted. In *B*, papain (10 nM), cathepsin L (10 nM), cathepsin G (40 nM), or HMC (10 nM) was incubated with SCCA1 (*closed circles*) or SCCA2 (*open circles*) at the indicated I_0/E_0 ratio. The residual enzyme activities are depicted. In *C*, after papain or cathepsin G was incubated with SCCA1 or SCCA2, the mixture was applied to SDS-PAGE. The gel stained by SYPRO Ruby is depicted. The *arrows* indicate SCCA1 (*), SCCA2 (**), and the complex of SCCA2 and cathepsin G (***).

these two proteins is unstable to SDS, like the complex between chymotrypsin and α_2-antiplasmin (21). To retain the native association between SCCA1 and papain, we employed a gel-filtration system. We subjected three different samples, whose I_0/E_0 ratios were 4.2, 5, and 6, for this analysis. It was confirmed that proteinase activities of papain were completely inhibited in the samples of $I_0/E_0 = 6$ and 5, but not 4.2 (data not shown). When these samples were applied to the gel-filtration column, most SCCA1 and papain were eluted according to their molecular weights (Fig. 2, *A–C*). However, an additional peak

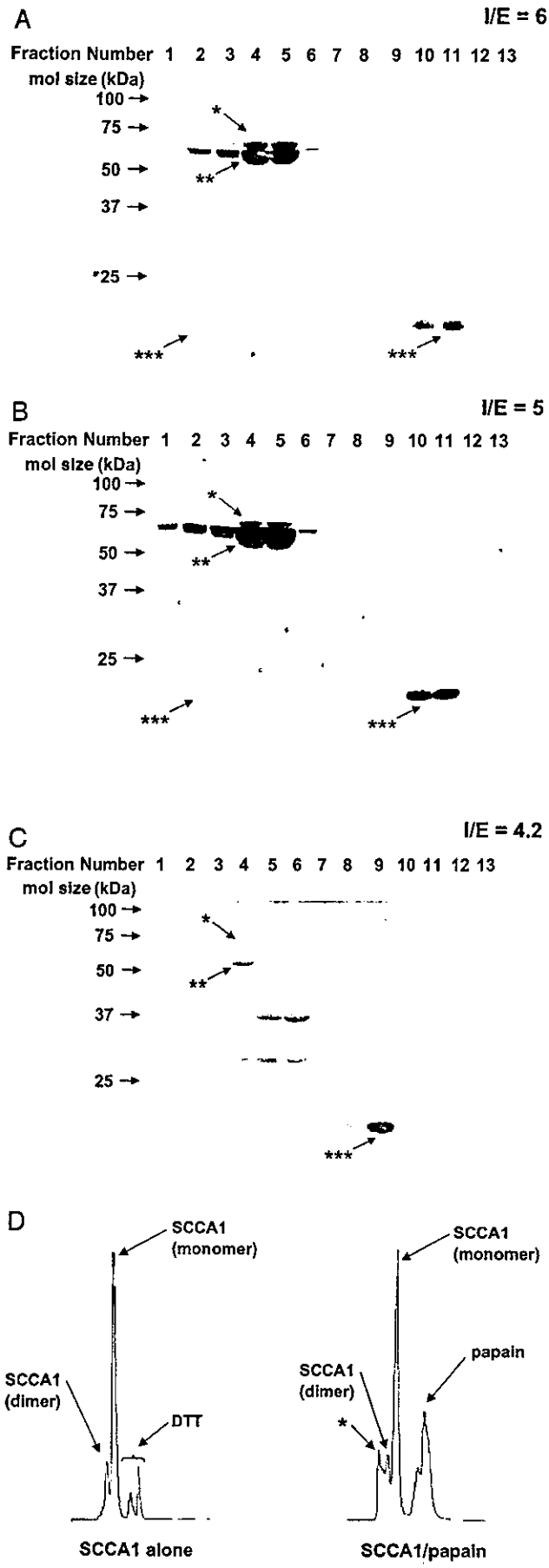

FIG. 2. **Elution profile of the reaction mixture of SCCA1 and papain by gel-filtration column.** The indicated concentrations of papain and 54 μM SCCA1 were incubated, and then the samples were applied to the gel-filtration column. Elution profile at I_0/E_0 = 6 (*A*), 5 (*B*), and 4.2 (*C*) stained by SYPRO Ruby is depicted. The *arrows* indicate intact (*) and truncated (**) SCCA1, as well as papain (***). In *D*, the chart showing the intensity of the absorbance at 280 nm of the eluted sample at I_0/E_0 = 6 is depicted. The *asterisk* indicates oligomers of SCCA1 and papain. *DTT*, dithiothreitol.

with a faster retention time was detected in the samples of I_0/E_0 = 6 and 5, but not 4.2, on the chart, although it was not detected when SCCA1 alone was applied (Fig. 2*D* and data not shown). Together with this peak on the chart, a band of low molecular weight the same as papain appeared on the SDS-PAGE gel in the samples of I_0/E_0 = 6 and 5, but not 4.2, as discussed later (Fig. 2, *A–C*). These results demonstrated that SCCA1 inhibited the catalytic activity of papain without forming a covalent bond.

Determination of the Cleavage Site in SCCA1 and Loss of Its Inhibitory Effect—It has been shown that the inhibitory serpins exert their activities by the suicide substrate-like inhibitory mechanism, in which the serpins interact with their target proteinases at their RSLs, which are then cleaved (2). We next investigated whether SCCA1 also used the inhibitory mechanism against papain as other serpins do. When papain-treated SCCA1 was eluted from the gel-filtration column, doublet bands appeared with molecular sizes of 62 and 55 kDa (Fig. 2, *A–C*). Both bands were recognized by anti-GST Ab, indicating that the upper and lower bands corresponded to intact and C-terminal truncated SCCA1, respectively (data not shown). We then determined the cleavage site of SCCA1 by papain, using amino acid sequencing and MALDI-TOF mass spectrometry. When we applied the visible band of <10 kDa to the amino acid sequencing, two sequences derived from SCCA1 were read out; the major one started at Ser-354, and the minor one started at Phe-352 (Fig. 3*A*). The measurement of papain-cleaved peptides in SCCA1 by MALDI-TOF mass spectrometry also revealed the existence of the peptide corresponding from Ser-354 to the C terminus and the peptide from Phe-352 to the C terminus, which was less than the peptide starting at Ser-354 (Fig. 3*B*). These results clearly demonstrated that the bond between Gly-353 and Ser-354 was the main cleavage site of SCCA1 and that the one between Gly-351 and Phe-352 was minor, as reported previously (13).

The intensities of the upper bands corresponding to intact SCCA1 became weaker as the I_0/E_0 ratio dropped, and those of the lower bands corresponding to truncated SCCA1 and of more degraded bands showed the opposite tendency (Fig. 2, *A–C*). If SCCA1 used the suicide mechanism, the inhibitory actions in these solutions would be parallel to the amount of intact SCCA1, irrespective of the amount of truncated SCCA1. To explore this possibility, after papain-treated SCCA1 was eluted by the gel-filtration column, we analyzed its inhibitory activity on freshly prepared papain. Consequently, the inhibitory activity of papain-treated SCCA1 increased parallel to the amount of intact SCCA (Fig. 4), which clearly supported the finding that the inhibitory manner of SCCA1 fit the suicide mechanism.

Association of Truncated SCCA1 and Papain—Although SCCA1 and papain did not form a covalent complex (Fig. 2, *A–C*), it was possible that the truncated SCCA1 would associate with papain non-covalently in the solution. Actually, an additional peak with a faster retention time than monomers or dimers of SCCA1 was detected by gel-filtration analysis, and a band of the same low molecular weight as papain appeared on the SDS-PAGE gel in the fractions corresponding to this peak (Fig. 2). It was reasonable to think that this fraction would correspond to co-migration of SCCA1-associated papain and truncated SCCA1. To explore this possibility, we first examined

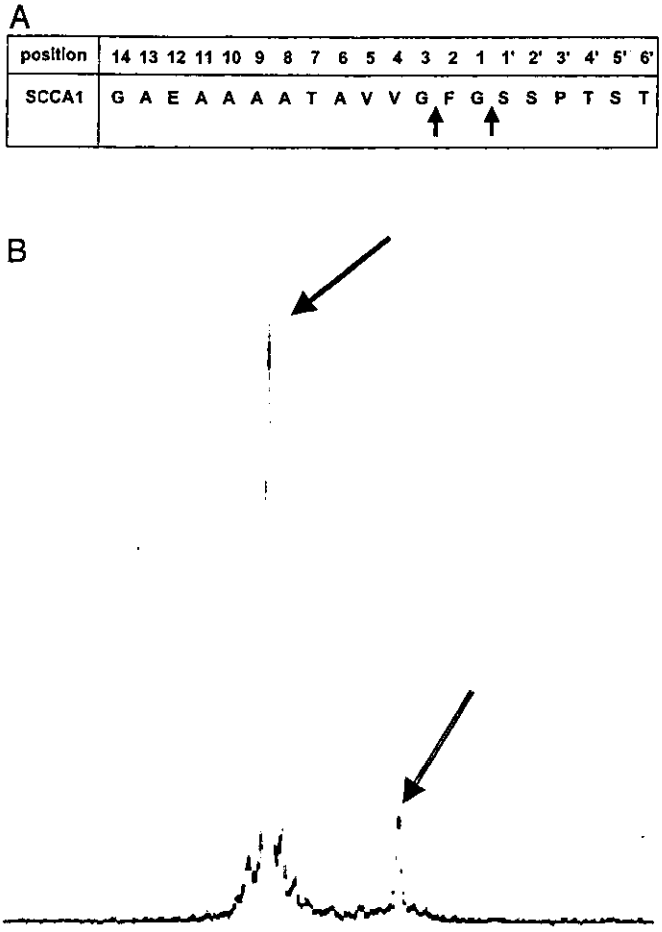

FIG. 3. **Cleavage site of SCCA1 by papain.** In *A*, the amino acid sequence of the RSL of SCCA1 is depicted. The *closed* and *open arrows* indicate the major and minor cleavage sites by papain identified by both the amino acid sequencing and MALDI-TOF mass spectrometry. In *B*, peaks of the cleaved C-terminal peptides identified by MALDI-TOF mass spectrometry are depicted. The *closed* and *open arrows* indicate the cleaved peptides as shown in *A*.

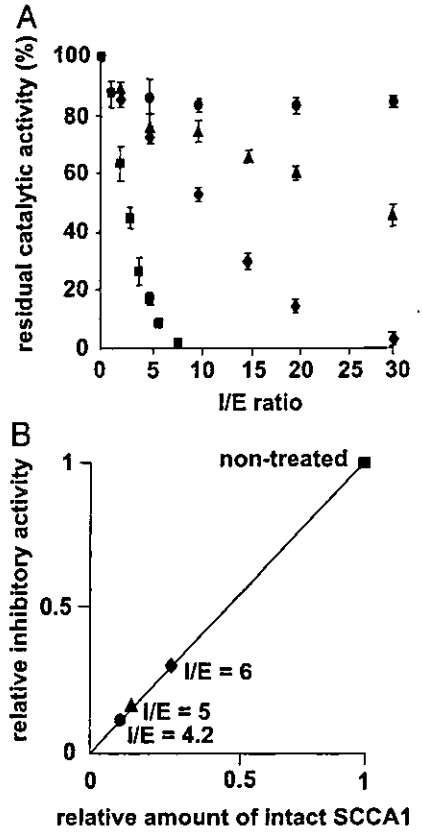

FIG. 4. **The catalytic activity of truncated SCCA1.** In *A*, a mixture of papain and SCCA1 prepared as described in the legend for Fig. 2 was applied to the gel-filtration column. Ten nM eluted SCCA1 (fraction 5 at I_0/E_0 = 5 and 6 and fraction 4 at I_0/E_0 = 4.2) was incubated with freshly prepared papain at the indicated I_0/E_0 ratio. The residual enzyme activity at the indicated I_0/E_0 ratio is depicted. In *B*, the relationship between the amount of intact SCCA1 of each sample and the intensity of the inhibitory activity is plotted. The amount of intact SCCA1 and the intensity of the inhibitory activity are estimated as the ratios of those of non-treated SCCA1 (*squares*).

whether the new peak was composed of SCCA1 and papain. Western blotting showed that the fractions corresponding to the peak with a faster retention time indicated the existence of papain (Fig. 5*A*). Both the peak on the chart and the band corresponding to papain in the Western blotting disappeared in the presence of an irreversible cysteine proteinase inhibitor, E-64 (Fig. 5, *B* and *C*). However, surprisingly, the molecular size of the complex was estimated as about 1100 kDa, judging from the retention time of the gel-filtration column (Fig. 5*D*), which is far larger than ~90 kDa, the expected molecular size of the 1:1 complex of papain and GST-fused SCCA1. These results suggested that although SCCA1 and papain formed a non-covalent complex dependent on the proteinase activity of papain, this complex was a huge molecule composed of several oligomers of SCCA1 and papain.

Although it was confirmed that papain and SCCA1 generated the relatively firmly associated complex of very large molecular weight, it was still possible that SCCA1-treated papain and truncated SCCA1 would form a transient, more loosely associated complex at 1:1 stoichiometry. To confirm the existence of such a complex, we next chemically cross-linked these two molecules by BS^3, which elicited the appearance of a 97-kDa band corresponding to a 1:1 complex composed of papain and truncated SCCA1 in the absence of E-64 (Fig. 6). This complex was recognized by both anti-papain and anti-GST Abs. A much fainter band with a bigger molecular size corresponding to the complex composed of papain and intact SCCA1 appeared in the presence of E-64. These results clearly suggested that SCCA1-treated papain and truncated SCCA1 formed a 1:1 complex dependent on the proteinase activity of papain in the reaction solution.

Preference of Amino Acids in RSL of SCCA1 for Papain—It is reasonable to assume that the distinct properties of SCCA1 and SCCA2 regarding the inhibitory effects on papain are due to the differences of their RSL sequences because only 7 amino acid residues among 13 (54%) are identical in the RSL regions (P7 to P6′) of these proteins (17). Actually, swapping the RSL of SCCA1 for that of SCCA2, or *vice versa*, revealed that the inhibitory effect on papain was dependent on the RSL of SCCA1 (SCCA1 RSL2, SCCA2 RSL1: Table I). We then exchanged each amino acid specific for the RSL of SCCA2 with that corresponding to SCCA1 and analyzed its inhibitory effect on papain (Table I). When Glu-353 was replaced with Gly, the mutated type showed the inhibitory effect at the same level as native SCCA1 (SCCA2 mut3). However, when Val-351, Val-352, or Leu-354 was replaced with Gly, Phe, or Ser, respectively, none of the mutated types exhibited the inhibitory effect (SCCA2 mut1, SCCA2 mut2, SCCA2 mut4). Furthermore, switching of both Ser-356 and Pro-357 with Pro and Thr, respectively, also did not recover the inhibitory activity (SCCA2 mut5). These results demonstrated that Gly-353 was critical for SCCA1 to exert its inhibitory effect on papain.

Irreversible Inhibition of SCCA1-treated Papain—We next examined whether SCCA1 treatment affects the catalytic ac-

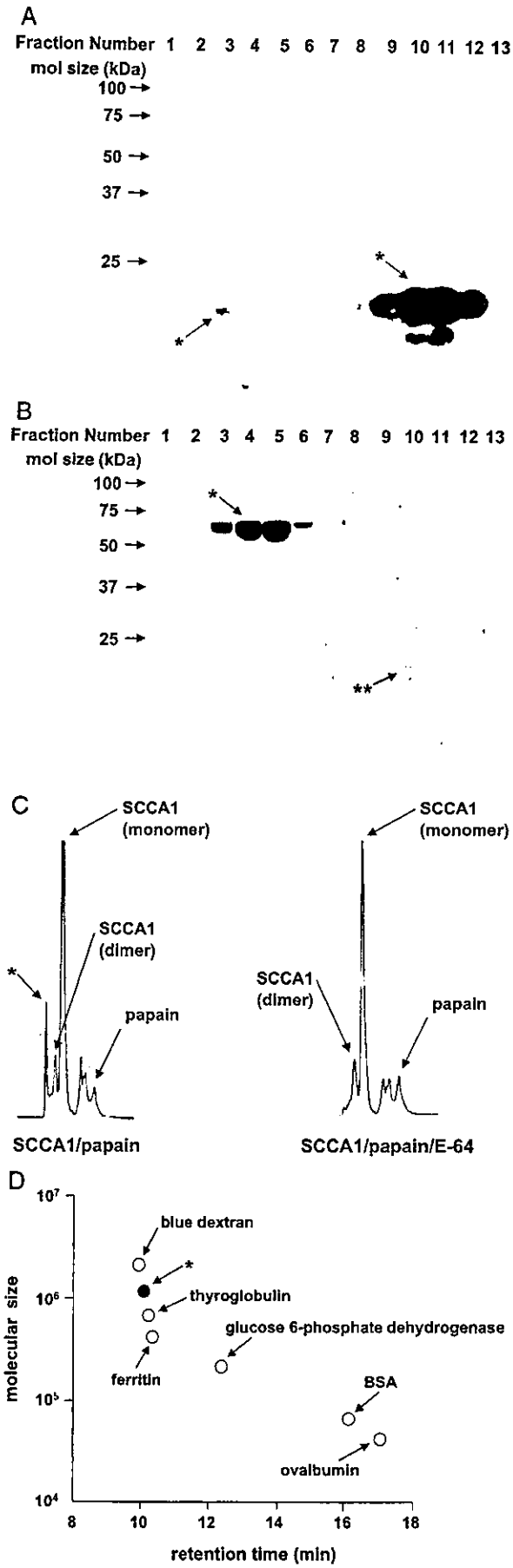

FIG. 5. **Co-migration of the SCCA1-treated papain and truncated SCCA1.** *A*, samples prepared as described in the legend for Fig. 2 in the absence of E-64 were applied to the gel-filtration column. The gel blotted by anti-papain Ab is depicted. *B*, samples prepared as described in the legend for Fig. 2 in the presence of E-64 were applied to the gel-filtration column. The gel stained with SYPRO Ruby is depicted. The *arrows* indicate intact SCCA1 (*) and papain (**). In *C*, the chart displaying the intensity of the absorbance at 280 nm is depicted. In *D*, retention time and molecular size of each protein are plotted. The *closed circle* (*) indicates the retention time and the estimated molecular weight of the oligomers of SCCA1 and papain. *BSA*, bovine serum albumin.

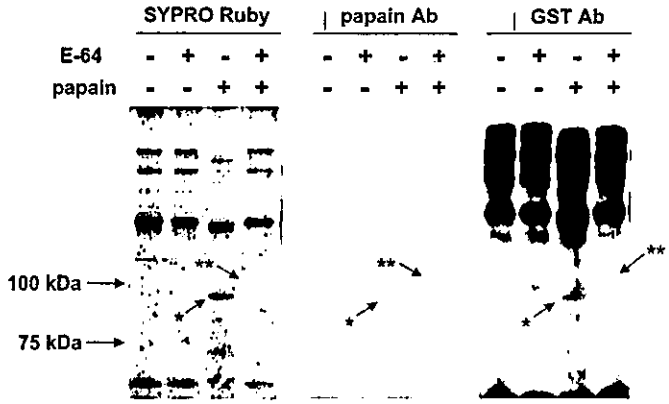

FIG. 6. **Chemical cross-linking of the associated SCCA1 and papain.** A mixture of 55 μM SCCA1 and 12 μM papain in the presence or absence of E-64 was incubated with BS^3, and then the samples were subjected to SDS-PAGE. Gels stained by SYPRO Ruby or blotted with anti-papain Ab or anti-GST Ab are depicted. The *arrows* indicate the complex of papain and either truncated (*) or intact (**) SCCA1.

tivity of papain. To address this question, we analyzed the proteinase activity of SCCA1-treated papain eluted by the gel-filtration column. We found that the proteinase activity of SCCA1-treated papain was severely impaired as compared with non-treated papain but was still present (15 ± 4.2% at I/E = 6, 17 ± 6.1% at I/E = 5, 20 ± 9.0% at I/E = 4.2, n = 3: Fig. 7*A*). The activity of E-64-treated papain was completely inhibited (2.7 ± 2.4%, n = 3). The K_m value of SCCA1-treated papain was more than that of non-treated papain (36.2 ± 1.35 μM, n = 3, p = 0.001), and the k_{cat} value of SCCA1-treated papain was less than that of non-treated papain (5.14 ± 0.202 s^{-1}, n = 3, p = 0.00008), which confirmed the impairment of the catalytic activity.

It is possible that, due to unexpected modification of the active cysteine residue of papain, SCCA1 treatment caused a significant decrease in its proteinase activity. To exclude this possibility, we compared modification of the active cysteine residue of SCCA1-treated or non-treated papain by biotin-conjugated maleimide. When non-treated papain was incubated with 77 μM maleimide for 2 h, its modification was not saturated (data not shown). Under this condition, modification of SCCA1-treated papain by biotin-conjugated maleimide was almost at the same level as non-treated papain (Fig. 7*B*). These results suggested that the active cysteine residue of papain was intact even after SCCA1 treatment. Taken together, these results suggest that SCCA1 treatment probably induced irreversible conformational change of papain, which severely impaired its proteinase activity.

Although SCCA1-treated papain still sustained its catalytic activity with the compromised level, all activity was abolished in the reactive solution (Figs. 1*B* and 7*A*). This may be due to the suicide substrate-like inhibition on the residual activity of papain by intact SCCA1. If this were the case, the catalytic activity of papain would be completely inhibited, whereas intact SCCA1 would remain. To explore this possibility, we analyzed the time-dependent profile of the proteinase activity of papain and the digestion pattern of SCCA1 (Fig. 8). Incubation

TABLE I
Alignment of RSLs of SCCA proteins and their inhibitory activities

Position	Proximal hinge							Reactive site loop											Distal hinge	Inhibition
	14	13	12	11	10	9	8	7	6	5	4	3	2	1	1′	2′	3′	4′	5′	6′	11′	
SCCA1	G	A	E	A	A	A	A	T	A	V	V	G	F	G	S	S	P	T	S	T	H	+
SCCA2	G	V	E	A	A	A	A	T	A	V	V	V	V	E	L	S	S	P	S	T	C	−
SCCA2 RSL1	.	A	.	.	.	.	.	.	.	.	.	G	F	G	S	.	P	T	.	.	H	+
SCCA1 RSL2	.	V	.	.	.	.	.	.	.	.	.	V	V	E	L	.	S	P	.	.	C	−
SCCA2 mut1(V351G)	.	V	.	.	.	.	.	.	.	.	.	G	V	E	L	.	S	P	.	.	C	−
SCCA2 mut2(V352F)	.	V	.	.	.	.	.	.	.	.	.	V	F	E	L	.	S	P	.	.	C	−
SCCA2 mut3(E353G)	.	V	.	.	.	.	.	.	.	.	.	V	V	G	L	.	S	P	.	.	C	+
SCCA2 mut4(L354S)	.	V	.	.	.	.	.	.	.	.	.	V	V	E	S	.	S	P	.	.	C	−
SCCA2 mut5(S356P P357T)	.	V	.	.	.	.	.	.	.	.	.	V	V	E	L	.	P	T	.	.	C	−

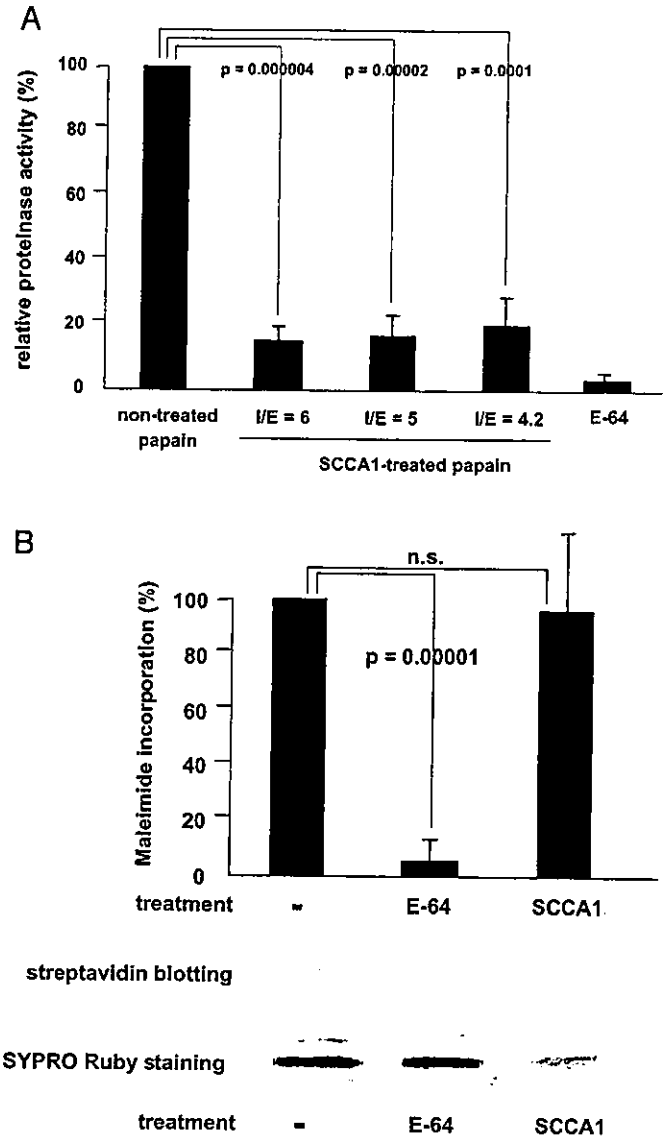

FIG. 7. **The catalytic activity of SCCA1-treated papain.** In *A*, the proteinase activities of SCCA1-treated, non-treated, or E-64-treated papain eluted as described in the legend for Fig. 2 are depicted. In *B*, SCCA1-treated or non-treated papain eluted as shown in *panel A* (0.4 μM) was incubated with 77 μM PEO-M-biotin. Blotting with horseradish peroxidase-conjugated streptavidin, SYPRO Ruby staining, and maleimide incorporation are shown. *n.s.*, not significant.

with SCCA1 led very quickly to complete inhibition of papain activity, lasting up to 2 h; however, the proteinase activity of papain started to recover at 4 h and then reached about 21% of the original activity at the same level as modified papain. In concert with the recovery of proteinase activity, the intact (62 kDa) and truncated (55 kDa) types of SCCA1 were completely degraded. These results indicated that if intact SCCA1 was completely cleaved by papain, the inhibitory effect of SCCA1 by the suicide substrate-like inhibition was no longer retained, allowing papain to recover its proteinase activity up to the lowest initial level.

DISCUSSION

In this article, we examined the inhibitory mechanism of a cross-class serpin, SCCA1, on papain. We propose the inhibition mechanism of SCCA1 as described in Fig. 9, as compared with the standard serpins (1, 2). In the standard serpins, a proteinase (*E*) and a serpin (*I*) initially form a non-covalent Michaelis-like complex (*EI*) followed by an acyl-enzyme intermediate (*EI**) linked by an oxy-ester bond. The inhibitory mechanism of SCCA1 on papain would share this pathway. In contrast, the acyl-enzyme intermediate (*EI**) is processed to either a covalent complex (EI^+), or a cleaved serpin (*I**) and a free proteinase (E) in the standard serpins. However, in the case of SCCA1, the acyl-enzyme intermediate (*EI**) linked by a thiol-ester bond would easily hydrolyze into the non-covalent complex (*E*I**) composed of cleaved SCCA1 (I*) and modified papain (*E**). Modified papain (*E**) loses most of its proteinase activity as compared with intact papain. Furthermore, a part of the non-covalent complex (*E*I**) forms a more firmly bound complex composed of oligomers ($E^*_mI^*_n$).

In this model, we first suggested that although SCCA1 used the suicide substrate-like mechanism as other serpins do, SCCA1 did not generate a covalent complex, in contrast to other serpins. The notion that SCCA1 used the suicide substrate-like mechanism was confirmed by the following results: 1) the RSL of SCCA1 was cleaved at the predicted site by papain (Fig. 3). 2) The inhibitory activity of SCCA1 on papain was dependent on intact, but not truncated, SCCA1 (Fig. 4). 3) Although intact SCCA1 existed, papain with a compromised level of proteinase activity lost its activity completely (Fig. 8). These results proved that the exposed RSL of SCCA1 was recognized by papain and that cleaved SCCA1 (I*) was inactive, which was in line with the typical suicide substrate-like mechanism. In contrast, a unique property of SCCA1 as a serpin has been also revealed. Most SCCA1 and papain were eluted according to their molecular weights by the gel-filtration column (Fig. 2), and truncated SCCA1 and papain formed a 1:1 complex dependent on the proteinase activity of papain (Fig. 6). These results indicated that the acyl-enzyme intermediate (EI^*) would be processed to formation of a non-covalent complex (E*I*) but not a covalent complex (EI^+). In the cleaved form of standard serpin, the insertion of RSL causes drastic conformational changes of the serpin and the proteinase so that the histidine residue of the catalytic triad was too far from the serine residue to let the ester bond hydrolyze (3). In the case of SCCA1, the partners of the catalytic center might still be close to the cysteine residue, making it possible for the ester bond to hydrolyze. It has been reported that other cross-class serpins, CrmA and PI9, also do not form SDS-resistant complexes with

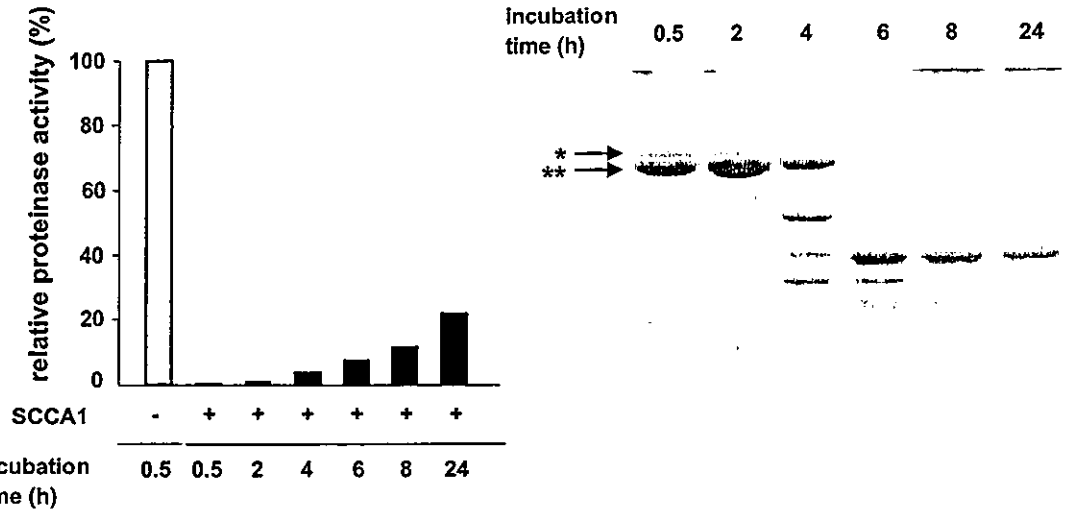

FIG. 8. **Time course profile of the reaction of papain and SCCA1.** SCCA1 (54.5 μM) was incubated with 10.9 μM papain for the indicated times at 25 °C, and the samples were applied to SDS-PAGE or the enzyme assay. The residual proteinase activities and the gel stained by SYPRO Ruby are depicted. The *arrows* indicate intact (*) and truncated (**) SCCA1.

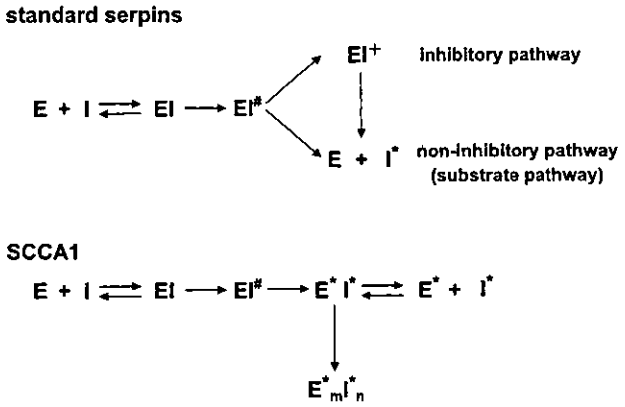

FIG. 9. **The schematic model of inhibition pathways of standard serpins and SCCA1.** The schematic model of inhibition pathways of standard serpins and SCCA1 is depicted. *E* and *I* represent proteinase (papain) and serpin (SCCA1), respectively. *EI*, *EI*#, *EI*$^+$, *E**, *I**, and $E^*_mI^*_n$ represent Michaelis-like complex, acyl-enzyme intermediate, covalent complex, modified papain, cleaved serpin, and oligomers of E* and I*, respectively. The inhibition pathway of standard serpins is based on Ref. 1.

caspase proteins (14, 16) as SCCA1 was unable to do with papain (Fig. 1*D*). Furthermore, we have recently observed that SCCA2 inhibited cysteine proteinase activity of a major mite allergen, Der p 1 and Der f 1, without forming a covalent complex.[2] Taking these results together, the suicide substrate-like mechanism, without forming a covalent complex, may be a common property of cross-class serpins. Thus far, it remains unresolved how stable the non-covalent complex (E*I*) would be. If this complex is not transient, but stable, formation of this complex would also contribute to the inhibition of free modified papain (E*) as the inhibitors of apoptosis protein family do for caspase proteins by partially substrate-like inhibition or as thrombin inhibitors do for thrombin by exosite binding inhibition (22, 23).

In this model, we next suggested that irreversible impairment of the catalytic activity of papain (E*) by SCCA1 contributed to the inhibitory mechanism of SCCA1 on papain, in addition to the suicide substrate-like mechanism (Fig. 9). This mechanism was verified by results that eluted papain showed compromised inhibitory activity (Fig. 7*A*) and that a longer exposure to SCCA1 allowed papain to recover its proteinase activity, but only up to the lowest initial level (Fig. 8). The contribution of the irreversible impairment to the whole inhibitory mechanism was significantly high (~85%: Fig. 7*A*). However, the result that incorporation of a thiol-residue modifying reagent, maleimide, into the SCCA1-treated papain was invariable with non-treated papain (Fig. 7*B*) suggested that SCCA1-treated papain still kept its conformation sufficiently for maleimide to access the catalytic cysteine residue. The drastic conformational change of a proteinase by engagement with its inhibitor is reported with the crystallographic structure between trypsin and α1-antitrypsin (3). The interaction of these two molecules causes a 37% loss of structure in trypsin; in particular, plucking of the ester-linked catalytic active center, Ser-195, from its catalytic partners prevents hydrolysis of the covalent bond, which sustains the complex. The result SCCA1 caused irreversible impairment of the catalytic activity of papain indicated that SCCA1 also disrupted the papain structure, as did the standard serpins. However, we also showed that incorporation of maleimide into papain was not affected, in addition to the result that the thiol-ester bond between SCCA1 and papain was unstable. These two results suggested that the distortion of papain induced by SCCA1 was not so complete (as is the case with standard serpins) that hydrolysis of the thiol-ester bond in cooperation with catalytic partners might still be possible.

Unexpectedly, in addition to a 1:1 complex, a part of truncated SCCA1 and SCCA1-treated papain formed a large complex composed of oligomers ($E^*_mI^*_n$) (Fig. 5). This complex was predicted to contain more than 10 molecules of SCCA1 and papain, although its precise components were unclear. As the formation of this complex disappeared with addition of E-64, intact SCCA1 (I) and papain (E) could not generate this complex (Fig. 5, *B* and *C*). It was speculated that truncated SCCA1 and SCCA1-treated papain changed their conformations so that the aberrant association between these two molecules might be induced.

We demonstrated that Gly-353 in the RSL was critical for the inhibitory effects of SCCA1 and that residue was sufficient for SCCA2 to achieve the same inhibitory effect as SCCA1 (Table I). The significance of the P1 residue of SCCA molecules is variable among the target proteinases. Glu-353 in SCCA2 was

[2] Y. Sakata, K. Arima, T. Takai, W. Sakurai, K. Masumoto, N. Yuyama, Y. Suminami, F. Kishi, T. Kato, H. Ogawa, K. Fujimoto, Y. Matsuo, Y. Sugita, and K. Izuhara, unpublished data.

important for the inhibitory effect on cathepsin G, whereas Gly-353 in SCCA1 was not required for the inhibitory effect on cathepsin S (17). When SCCA1 and papain interact, Gly-353 locates deep at the cleft of papain and forms a thiol-ester bond with Cys-25 of papain. It may be that the ionic strength of Glu interrupts the interaction of the RSL and papain, whereas Gly at the P1 site stabilizes the interaction.

As it is widely known that proteinases play important roles in the homeostasis of the body, proteinase inhibitors have great potential as novel therapeutic reagents. Cathepsin S degrades the invariant chain, important for antigen presentation of major histocompatibility class II molecules so that cathepsin S-deficient mice show diminished susceptibility to collagen-induced arthritis (24, 25). Cathepsin K is involved in bone remodeling by degrading bone matrix proteins such as type I and type II collagen, and the loss-of-function mutations in the cathepsin K gene evoke pycnodysostosis, characterized by osteosclerosis and short stature (26–28). Cathepsin L is reported to have a critical role for degrading invariant chain as well as cathepsin L (29); however, the analyses of cathepsin L-deficient mice show that unexpectedly, cathepsin L is important for epidermal homeostasis and hair follicle morphogenesis (30). Because SCCA1 has an ability to inhibit all of these proteinases, the compounds that mimic the inhibitory effects of SCCA1 have the potential to be applied to autoimmune diseases, osteoporosis, and epidermal disorder diseases (30, 31). Furthermore, we have recently demonstrated that expression of SCCA1 is related to bronchial asthma, although it has remained unresolved whether it acts as a worsening or preventing factor (11). It would be of use for developing a therapeutic reagent against these diseases to clarify the precise mechanism of the inhibitory mechanism of SCCA1. In conclusion, we show in this article that SCCA1 inhibits the catalytic activity of papain in two ways, contributing the suicide substrate-like mechanism without formation of a covalent complex and causing irreversible impairment of papain.

Acknowledgments—We thank Dr. Dovie R. Wylie for critical review of this manuscript. We also thank Drs. Yoshinori Suminami, Fumio Kishi, Yoshito Abe, and Toshihiro Kondo for providing the plasmids coding SCCA1 and SCCA2 and technical support.

REFERENCES

1. Silverman, G. A., Bird, P. I., Carrell, R. W., Church, F. C., Coughlin, P. B., Gettins, P. G., Irving, J. A., Lomas, D. A., Luke, C. J., Moyer, R. W., Pemberton, P. A., Remold-O'Donnell, E., Salvesen, G. S., Travis, J., and Whisstock, J. C. (2001) *J. Biol. Chem.* **276,** 33293–33296
2. Ye, S., and Goldsmith, E. J. (2001) *Curr. Opin. Struct. Biol.* **11,** 740–745
3. Huntington, J. A., Read, R. J., and Carrell, R. W. (2000) *Nature* **407,** 923–926
4. Schick, C., Kamachi, Y., Bartuski, A. J., Cataltepe, S., Schechter, N. M., Pemberton, P. A., and Silverman, G. A. (1997) *J. Biol. Chem.* **272,** 1849–1855
5. Schneider, S. S., Schick, C., Fish, K. E., Miller, E., Pena, J. C., Treter, S. D., Hui, S. M., and Silverman, G. A. (1995) *Proc. Natl. Acad. Sci. U. S. A.* **92,** 3147–3151
6. Kato, H., and Torigoe, T. (1977) *Cancer (Phila.)* **40,** 1621–1628
7. Cataltepe, S., Gornstein, E. R., Schick, C., Kamachi, Y., Chatson, K., Fries, J., Silverman, G. A., and Upton, M. P. (2000) *J. Histochem. Cytochem.* **48,** 113–122
8. Suminami, Y., Nagashima, S., Vujanovic, N. L., Hirabayashi, K., Kato, H., and Whiteside, T. L. (2000) *Br. J. Cancer* **82,** 981–989
9. Murakami, A., Suminami, Y., Hirakawa, H., Nawata, S., Numa, F., and Kato, H. (2001) *Br. J. Cancer* **84,** 851–858
10. McGettrick, A. F., Barnes, R. C., and Worrall, D. M. (2001) *Eur. J. Biochem.* **268,** 5868–5875
11. Yuyama, N., Davies, D. E., Akaiwa, M., Matsui, K., Hamasaki, Y., Suminami, Y., Lu Yoshida, N., Maeda, M., Pandit, A., Lordan, J. L., Kamogawa, Y., Arima, K., Nagumo, F., Sugimachi, M., Berger, A., Richards, I., Roberds, S. L., Yamashita, T., Kishi, F., Kato, H., Arai, K., Ohshima, K., Tadano, J., Hamasaki, N., Miyatake, S., Sugita, Y., Holgate, S. T., and Izuhara, K. (2002) *Cytokine* **19,** 287–296
12. Takeda, A., Yamamoto, T., Nakamura, Y., Takahashi, T., and Hibino, T. (1995) *FEBS Lett.* **359,** 78–80
13. Schick, C., Pemberton, P. A., Shi, G. P., Kamachi, Y., Cataltepe, S., Bartuski, A. J., Gornstein, E. R., Bromme, D., Chapman, H. A., and Silverman, G. A. (1998) *Biochemistry* **37,** 5258–5266
14. Komiyama, T., Ray, C. A., Pickup, D. J., Howard, A. D., Thornberry, N. A., Peterson, E. P., and Salvesen, G. (1994) *J. Biol. Chem.* **269,** 19331–19337
15. Zhou, Q., Snipas, S., Orth, K., Muzio, M., Dixit, V. M., and Salvesen, G. S. (1997) *J. Biol. Chem.* **272,** 7797–7800
16. Annand, R. R., Dahlen, J. R., Sprecher, C. A., De Dreu, P., Foster, D. C., Mankovich, J. A., Talanian, R. V., Kisiel, W., and Giegel, D. A. (1999) *Biochem. J.* **342,** 655–665
17. Luke, C., Schick, C., Tsu, C., Whisstock, J. C., Irving, J. A., Bromme, D., Juliano, L., Shi, G. P., Chapman, H. A., and Silverman, G. A. (2000) *Biochemistry* **39,** 7081–7091
18. Quan, L. T., Caputo, A., Bleackley, R. C., Pickup, D. J., and Salvesen, G. S. (1995) *J. Biol. Chem.* **270,** 10377–10379
19. Bird, C. H., Sutton, V. R., Sun, J., Hirst, C. E., Novak, A., Kumar, S., Trapani, J. A., and Bird, P. I. (1998) *Mol. Cell. Biol.* **18,** 6387–6398
20. Melo, R. L., Barbosa Pozzo, R. C., Alves, L. C., Perissutti, E., Caliendo, G., Santagada, V., Juliano, L., and Juliano, M. A. (2001) *Biochim. Biophys. Acta* **1547,** 82–94
21. Enghild, J. J., Valnickova, Z., Thogersen, I. B., Pizzo, S. V., and Salvesen, G. (1993) *Biochem. J.* **291,** 933–938
22. Stennicke, H. R., Ryan, C. A., and Salvesen, G. S. (2002) *Trends Biochem. Sci.* **27,** 94–101
23. Bode, W., and Huber, R. (2000) *Biochim. Biophys. Acta* **1477,** 241–252
24. Shi, G. P., Villadangos, J. A., Dranoff, G., Small, C., Gu, L., Haley, K. J., Riese, R., Ploegh, H. L., and Chapman, H. A. (1999) *Immunity* **10,** 197–206
25. Nakagawa, T. Y., Brissette, W. H., Lira, P. D., Griffiths, R. J., Petrushova, N., Stock, J., McNeish, J. D., Eastman, S. E., Howard, E. D., Clarke, S. R., Rosloniec, E. F., Elliott, E. A., and Rudensky, A. Y. (1999) *Immunity* **10,** 207–217
26. Gelb, B. D., Shi, G. P., Chapman, H. A., and Desnick, R. J. (1996) *Science* **273,** 1236–1238
27. Saftig, P., Hunziker, E., Wehmeyer, O., Jones, S., Boyde, A., Rommerskirch, W., Moritz, J. D., Schu, P., and von Figura, K. (1998) *Proc. Natl. Acad. Sci. U. S. A.* **95,** 13453–13458
28. Hou, W. S., Bromme, D., Zhao, Y., Mehler, E., Dushey, C., Weinstein, H., Miranda, C. S., Fraga, C., Greig, F., Carey, J., Rimoin, D. L., Desnick, R. J., and Gelb, B. D. (1999) *J. Clin. Invest.* **103,** 731–738
29. Nakagawa, T., Roth, W., Wong, P., Nelson, A., Farr, A., Deussing, J., Villadangos, J. A., Ploegh, H., Peters, C., and Rudensky, A. Y. (1998) *Science* **280,** 450–453
30. Roth, W., Deussing, J., Botchkarev, V. A., Pauly-Evers, M., Saftig, P., Hafner, A., Schmidt, P., Schmahl, W., Scherer, J., Anton-Lamprecht, I., Von Figura, K., Paus, R., and Peters, C. (2000) *FASEB J.* **14,** 2075–2086
31. Leung-Toung, R., Li, W., Tam, T. F., and Karimian, K. (2002) *Curr. Med. Chem.* **9,** 979–1002